8. THREE-PHASE SYNCHRONOUS MACHINE

Co-author: V. Brandwajn

The details with which synchronous machines must be modelled depend very much on the type of transient study. Most readers will be familiar with the simple representation of the synchronous machine as a voltage source E" behind a subtransient reactance X_d". This representation is commonly used in short-circuit studies with steady-state phasor solutions, and is also reasonably accurate for transient studies for the first few cycles of a transient disturbance. Switching surge studies fall into that category. Another well-known representation is E' behind X_d' for simplified stability studies. Both of these representations can be derived from the same detailed model by making certain assumptions, such as neglecting flux linkage changes in the field structure circuits for E" behind X_d", and in addition, assuming that the damper winding currents have died out for E' behind X_d'.

The need for the detailed model described here arose in connection with subsynchronous resonance studies in the mid-1970's. In such studies, the time span is too long to allow the use of simplified models. Furthermore, the torsional dynamics of the shaft with its generator rotor and turbine rotor masses had to be represented as well. Detailed models are now also used for other types of studies (e.g., simulation of out-of-step synchronization). To cover all possible cases, the synchronous machine model represents the details of the electrical part of the generator as well as the mechanical part of the generator and turbine. For studies in which speed variations and torsional vibrations can be ignored, an option is provided for by-passing the mechanical part of the UBC EMTP.[1]

The synchronous machine model was developed for the usual design with three-phase ac armature windings on the stator and a dc field winding with one or more pole pairs on the rotor. For a reversed design (armature windings on the rotor and field winding on the stator), it is probably possible to represent the machine in some equivalent way as a machine with the usual design. Even though the model was developed with turbine-driven generators in mind, it can be used for synchronous motors as well (e.g., pumping mode in a pumped-storage plant).

The model cannot be used for dual-excited machines (one field winding in direct axis and another field winding in quadrature axis) at this time, thought it would be fairly easy to change the program to allow for it. Since such machines have not yet found practical acceptance, it was felt that the extra programming was not justified. Induction machines can also not be modelled with it, though program changes could again be made for that purpose. For these and other types of machines, the universal machine of Section 9 should be used.

While the equations for the detailed machine model have been more or less the same in all attempts to incorporate them into the EMTP, there have been noticeable differences in how their solution is interfaced with the rest of the network. K. Carlsen, E.H. Lenfest and J.J. LaForest were probably the first to add a machine model to the EMTP, but the resulting "MANTRAP" - program [97] was not made available to users outside General Electric Co. M.C. Hall, J. Alms (Southern California Edison Co.) and G. Gross (Pacific Gas & Electric Co.), with the assistance of W.S. Meyer (Bonneville Power Administration), implemented the first model which became available

[1]The synchronous machine model is the UBC EMTP is experimental and has not been released.

to the general public. They opted for an iterative solution at each time step, with the rest of the system, as seen from the machine terminals, represented by a three-phase Thevenin equivalent circuit [98]. To keep this "compensation" approach efficient, machines had to be separated by distributed-parameter lines from each other. If that separation did not exist in reality, short artificial "stub lines" had to be introduced which sometimes caused problems. V. Brandwajn suggested another alternative in which the machine is basically represented as an internal voltage source behind some impedance. The voltage source is recomputed for each time step, and the impedance becomes part of the nodal conductance matrix [G] in Eq. (1.8). This approach depends on the prediction of some variables, which are not corrected at one and the same time step in order to keep the algorithm non-iterative. While the prediction can theoretically cause numerical instability, it has been refined to such an extent by now that the method has become quite stable and reliable. Whether an option for repeat solutions as correctors will be added someday remains to be seen. Numerical stability has been more of a problem with machine models partly because the typical time span of a few cycles in switching surge studies has grown to a few seconds in machine transient studies, with the step size Δt being only slightly larger, if at all, in the latter case.

8.1 Basic Equations for Electrical Part

Since there is no uniformity on sign conventions in the literature, the sign conventions used here shall first be summarized:

(a) The flux linkage λ of a winding, produced by current in the same winding, is considered to have the same sign as the current ($\lambda = Li$, with L being the self inductance of the winding).

(b) The "generator convention" is used for all windings, that is, each winding k is described by

$$v_k(t) = -R_k\, i_k(t) - \frac{d\lambda_k(t)}{dt} \tag{8.1}$$

(with the "load convention," the signs would be positive on the right-hand side).

(c) The newly recommended position of the quadrature axis lagging 90° behind the direct axis in the machine phasor diagram is adopted here [99]. In Park's original work, and in most papers and books, it is leading, and as a consequence the terms in the second row of $[T]^{-1}$ of Eq. (8.7b) have negative signs there.

The machine parameters are influenced by the type of construction. Salient-pole machines are used in hydro plants, with 2 or more (up to 50) pole pairs. The magnetic properties of a salient-pole machine along the axis of symmetry of a field pole (direct axis) and along the axis of symmetry midway between two field poles (quadrature axis) are noticeably different because a large part of the path in the latter case is in air (Fig. 8.1a). Cylindrical-rotor machines have long cylindrical rotors with slots in which distributed field windings are placed (Fig. 8.1b). They are used in thermal plants, and have 1 or 2 pole pairs. For cylindrical-rotor machines the magnetic properties on the two axes differ only slightly (because of the field windings embedded in the slots), and this difference ("saliency") can often be ignored. The word saliency is used as a short expression for the fact that the rotor has

different magnetic properties on the two axes.

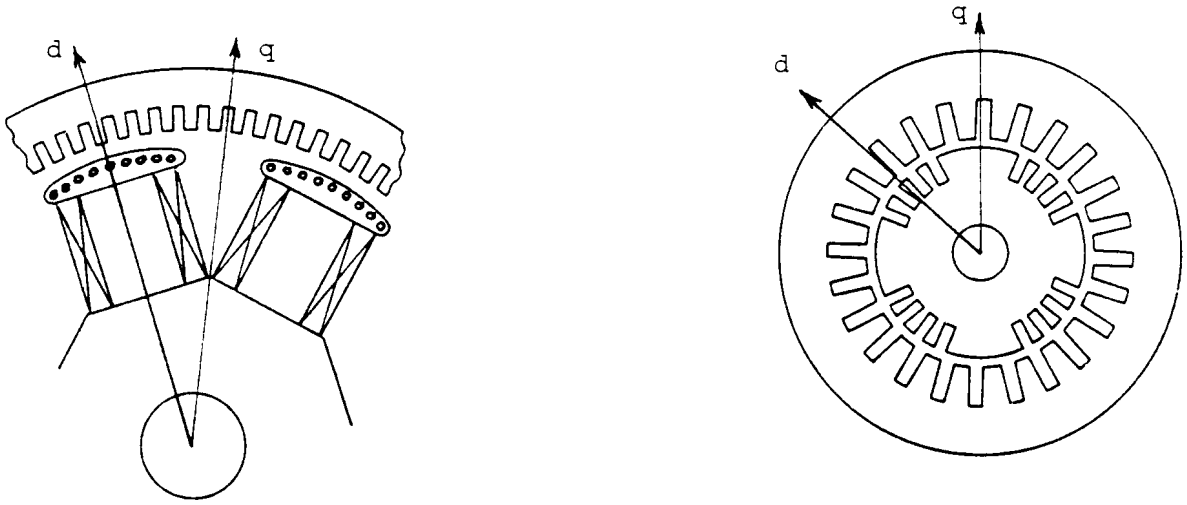

(a) Salient-pole machine (b) Cylindrical-rotor machine

Fig. 8.1 - Cross sections of synchronous machines (d = direct axis, q = quadrature axis) [101]. Reprinted by permission of I. Kimbark

The machine model in the EMTP always allows for saliency; if saliency is ignored, the same equations will still be used, except that certain parameters will have been set equal at input time ($X_q = X_d$, etc.).

The electrical part of the synchronous machine is modelled as a two-pole machine with 7 coupled windings[2]:

1
2 three armature windings (connected to the power system),
3

f one field winding which produces flux in the direct axis (connected to the dc source of the excitation system),

g one hypothetical winding in the quadrature axis to represent slowly changing fluxes in the quadrature axis which are produced by deep-flowing eddy currents (normally negligible in salient-pole machines)

D one hypothetical winding in the direct axis to represent damper bar effects,

Q one hypothetical winding in the quadrature axis to represent damper bar effects.

For machines with more than one pole-pair, the electrical equations are the same as for one pole-pair, except that the angular frequency and the torque being used in the equations of the mechanical part must be converted as follows:

---

[2]Another, more modern approach is to measure the frequency response from the terminals, which can then be used to represent the machine with transfer functions between the terminals, without assuming a given number of lumped windings a priori. One can also use curve fitting techniques to match this measured response with that from a series and parallel combination of R-L branches [100]. The end results in the latter case is basically the same model as described here, except that damper bars are sometimes represented by more than one winding, and that the data is obtained from frequency response tests.

$$\omega_{actual} = \frac{\omega_{2\text{-}pole\text{-}machine}}{p/2} \tag{8.2a}$$

$$T_{actual} = \frac{p}{2} T_{2\text{-}pole\text{-}machine} \tag{8.2b}$$

where p/2 is the number of pole pairs.

The behavior of the 7 windings is described by two systems of equations, namely by the voltage equations

$$[v] = -[R][i] - \frac{d}{dt}[\lambda] \tag{8.3}$$

with

$[i] = [i_1, i_2, i_3, i_f, i_g, i_D, i_Q]$,

$[\lambda] = [\lambda_1, \lambda_2, \lambda_3, \lambda_f, \lambda_g, \lambda_D, \lambda_Q]$,

$[v] = [v_1, v_2, v_3, v_f, 0, 0, 0]$ (zero in last 3 components because g-, D-, and Q- windings are short-circuited)

$[R] =$ diagonal matrix of winding resistances $R_a, R_a, R_a, R_f, R_g, R_D, R_Q$ (subscript "a" for armature),

and by the flux-current relationship

$$[\lambda] = [L][i] \quad with\ [L] = \begin{bmatrix} L_{11} & L_{12} & \dots & L_{1Q} \\ L_{21} & L_{22} & \dots & L_{2Q} \\ . & . & . & . \\ L_{Q1} & L_{Q2} & \dots & L_{QQ} \end{bmatrix} \tag{8.4}$$

To make the equations manageable, a number of idealized characteristics are assumed, which are reasonable for system studies. These assumptions for the "ideal synchronous machine" [76, p. 700] are[3]:

(1) The resistance of each winding is constant.

(2) The permeance of each portion of the magnetic circuit is constant (corrections for saturation effects will be introduced later, however).

(3) The armature windings are symmetrical with respect to each other.

(4) The electric and magnetic circuits of the field structure are symmetrical about the direct or quadrature axis.

(5) The self inductance of each winding on the field structure (f, g, D, Q) is constant.

(6) The self and mutual inductances of the armature windings are a constant plus a second-harmonic sinusoidal function of the rotor position β (second-harmonic component zero if saliency ignored), with the amplitude of the second-harmonic component being the same for all self and mutual

[3]For a detailed design analysis of synchronous machines, many of these idealizations cannot be made. Since they imply that the field distribution across a pole is a fundamental sinusoid, harmonics produced by the nonsinusoidal field distribution in a real machine could not be studied with the ideal machine implemented in the EMTP.

inductances.

(7) The mutual inductance between any winding on the field structure and any armature winding is a fundamental sinusoidal function of the rotor position β.

(8) Effects of hysteresis are negligible.

(9) Effects of eddy currents are negligible or, in the case of cylindrical-rotor machines, are represented by the g-winding.

Then,

$$\begin{gathered} L_{11} = L_s + L_m\cos 2\beta, \qquad similar for L_{22},\ L_{33} \\ L_{12} = L_{21} = M_s + L_m\cos(2\beta - 120°) \quad similar\ for\ L_{13},\ L_{23} \\ L_{1f} = L_{f1} = M_{af}\cos\beta \qquad similar\ for\ L_{2f},\ L_{3f} \\ L_{1D} = L_{D1} = M_{aD}\cos\beta \qquad similar\ for\ L_{2D},\ L_{3D} \\ L_{1g} = L_{g1} = M_{ag}\sin\beta \qquad similar\ for\ L_{2g},\ L_{3g} \\ L_{1Q} = L_{Q1} = M_{aQ}\sin\beta \qquad similar\ for\ L_{2Q},\ L_{3Q} \\ L_{ff},\ L_{gg},\ L_{DD},\ L_{QQ},\ M_{fD},\ M_{gQ} \quad constant \quad (not\ functions\ of\ \beta) \end{gathered} \tag{8.5}$$

with β being the angular position of the assumed two-pole rotor relative to the stator ($\beta_{actual} = \beta_{2\text{-pole-machine}} / p/2$), which is related to the angular frequency,

$$\omega = \frac{d\beta}{dt} \tag{8.6}$$

Some authors (e.g., Kimbark [101]) use a different sign for M_s in Eq. (8.5). With the sign used here, the numerical value will be negative.

The solution of the two systems of equations (8.3) and (8.4) is complicated by the fact that the inductances in Eq. (8.4) are functions of time through their dependence on β in Eq. (8.5). While it is possible to solve them directly in phase quantities[4], most authors prefer to transform them from phase quantities to d, q, 0- quantities because the inductances become constants in the latter reference frame. This transformation projects the rotating fluxes onto the field axis, from where they appear as stationary during steady-state operation. The transformation was first proposed by Blondel, and further developed by Doherty, Nickle and Park; in North America, it is now often called Park's transformation. The transformation is identical for fluxes, voltages, and currents, and converts phase quantities 1, 2, 3 into d, q, 0- quantities, with quantities on the field structure remaining unchanged,

$$[\lambda_{dq0}] = [T]^{-1}[\lambda] \qquad identical\ for\ [v],\ [i] \tag{8.7a}$$

with

[4]If space harmonics in the magnetic field distribution had to be taken into account, then L_{11} and L_{12} in Eq. (8.5) would have added 4th, 6th, and higher harmonics terms, and L_{1f} etc. would have added 3rd, 5th,…harmonics terms. In that case, solutions in phase quantities would probably be the best choice.

$$[\lambda_{dq0}] = [\lambda_d,\ \lambda_q,\ \lambda_0,\ \lambda_f,\ \lambda_g,\ \lambda_D,\ \lambda_Q]\ , \quad \textit{and}$$

Remain unchanged

$$[T]^{-1} = \begin{bmatrix} \frac{\sqrt{2}}{\sqrt{3}}\cos\beta & \frac{\sqrt{2}}{\sqrt{3}}\cos(\beta-120°) & \frac{\sqrt{2}}{\sqrt{3}}\cos(\beta+120°) & 0 & 0 & 0 & 0 \\ \frac{\sqrt{2}}{\sqrt{3}}\sin\beta & \frac{\sqrt{2}}{\sqrt{3}}\sin(\beta-120°) & \frac{\sqrt{2}}{\sqrt{3}}\sin(\beta+120°) & 0 & 0 & 0 & 0 \\ \frac{1}{\sqrt{3}} & \frac{1}{\sqrt{3}} & \frac{1}{\sqrt{3}} & 0 & 0 & 0 & 0 \\ 0 & 0 & 0 & 1 & 0 & 0 & 0 \\ 0 & 0 & 0 & 0 & 1 & 0 & 0 \\ 0 & 0 & 0 & 0 & 0 & 1 & 0 \\ 0 & 0 & 0 & 0 & 0 & 0 & 1 \end{bmatrix} \tag{8.7b}$$

Eq. (8.7) is an orthogonal transformation; it therefore follows that

$$[T] = [T]^{-1}_{transposed} \tag{8.8}$$

The matrices [T] and $[T]^{-1}$ are normalized here. This has the advantage that the power is invariant under transformation, and more importantly, that the inductance matrix in d, q, 0- quantities is always symmetric. The lack of symmetry with unnormalized quantities can easily lead to confusion, because it is often removed by rescaling of field structure quantities which in turn imposes unnecessary restrictions on the choice of base values if p.u. quantities are used. Authors who work with unnormalized transformations use a factor 2/3 in the first two rows of Eq. (8.7b), and 1/3 in the third row. In many older publications the position of the quadrature axis is assumed 90° ahead of the direct axis, rather than lagging 90° behind d-axis as here, and the second row of Eq. (8.7b) has therefore negative signs there.

Transforming Eq. (8.3) to d, q, 0- quantities yields

$$[v_{dq0}] = -[R]\,[i_{dq0}] - \frac{d}{dt}[\lambda_{dq0}] + \begin{bmatrix} -\omega\lambda_q \\ +\omega\lambda_d \\ 0 \\ 0 \\ 0 \\ 0 \\ 0 \end{bmatrix} \tag{8.9}$$

which is almost identical in form to Eq. (8.3), except for the "speed voltage terms" $-\omega\lambda_q$ and $\omega\lambda_d$ (voltage induced

in armature because of rotating field poles). They come out of Eq. (8.3) by keeping in mind that [T] is a function of time,

$$[T]^{-1}\frac{d}{dt}\{[T][\lambda_{dq0}]\} = \frac{d}{dt}[\lambda_{dq0}] + [T]^{-1}\left\{\frac{d}{dt}[T]\right\}[\lambda_{dq0}]$$

Transforming Eq. (8.4) yields flux-current relationships which can be partitioned into two systems of equations for the direct and quadrature axis, and one equation for zero sequence,

$$\begin{bmatrix}\lambda_d\\ \lambda_f\\ \lambda_D\end{bmatrix} = \begin{bmatrix}L_d & M_{df} & M_{dD}\\ M_{df} & L_{ff} & M_{fD}\\ M_{dD} & M_{fD} & L_{DD}\end{bmatrix}\begin{bmatrix}i_d\\ i_f\\ i_D\end{bmatrix} \qquad (8.10a)$$

$$\textit{where} \quad M_{df} = \frac{\sqrt{3}}{\sqrt{2}}M_{af}, \qquad M_{dD} = \frac{\sqrt{3}}{\sqrt{2}}M_{aD}$$

$$\begin{bmatrix}\lambda_q\\ \lambda_g\\ \lambda_Q\end{bmatrix} = \begin{bmatrix}L_q & M_{qg} & M_{qQ}\\ M_{qg} & L_{g\,g} & M_{gQ}\\ M_{qQ} & M_{gQ} & L_{QQ}\end{bmatrix}\begin{bmatrix}i_q\\ i_g\\ i_Q\end{bmatrix} \qquad (8.10b)$$

$$\textit{where} \quad M_{qg} = \frac{\sqrt{3}}{\sqrt{2}}M_{ag}, \qquad M_{qQ} = \frac{\sqrt{3}}{\sqrt{2}}M_{aQ}$$

$$\textit{and} \qquad \lambda_0 = L_0\, i_0 \qquad (8.10c)$$

Most elements of these inductance matrices with constant coefficients have already been defined in Eq. (8.5), except for

direct axis synchronous inductance $L_d = L_s - M_s + 3/2\ L_m$,

quadr. axis synchronous inductance $L_q = L_s - M_s - 3/2\ L_m$, (8.11)

zero sequence inductance $L_0 = L_s + 2M_s$.

8.2 Determination of Electrical Parameters[5]

[5]The assistance of S. Bhattacharya and Ye Zhong-liang in research for this section is gratefully acknowledged.

A set of resistances and of self and mutual inductances is needed in the two systems of equations (8.9) and (8.10), which are not directly available from calculations or measurements. According to IEEE or IEC standards [102, 103] the known quantities are

armature resistance	R_a,
armature leakage reactance	X_l,
zero sequence reactance	X_o,
transient reactances	X_d', X_q',
subtransient reactances	X_d'', X_q'',
transient short-circuit time constants	T_d', T_q',
subtransient short-circuit time constants	T_d'', T_q''.

All reactances and time constants must be unsaturated values, because saturation is considered separately, as explained in Section 8.6. This is the reason why short-circuit time constants are preferred as test data over open-circuit time constants, because the measurement of the latter is influenced by saturation effects [104]. Fortunately, one set of time constants can be converted precisely into the other set [104], as explained in Appendix VI in Eq. (VI. 14c) and (VI. 21),

$$T'_{d0} + T''_{d0} = \frac{X_d}{X_d'} T_d' + \left(1 - \frac{X_d}{X_d'} + \frac{X_d}{X_d''}\right) T_d''$$

$$T'_{d0} T''_{d0} = T_d' T_d'' \frac{X_d}{X_d''} \tag{8.12}$$

for the direct axis, and identically for the quadrature axis by replacing subscript "d" with "q."

The number of known parameters is less than the number of resistance and inductance values in Eq. (8.9) and (8.10), and some assumptions must therefore be made before the data can be converted. Since the procedure for data conversion is the same for the direct and quadrature axis parameters, only the direct axis will be discussed from here on.

Winding D is a hypothetical winding which represents the effects of the damper bar squirrel cage. We can therefore assume any number of turns for it, without loss of generality. In particular, we can choose the number of turns in such a way that

$$M_{dD} = M_{df} \tag{8.13a}$$

in Eq. (8.10a), and similarly

$$M_{qQ} = M_{qg} \tag{8.13b}$$

in Eq. (8.10b). Many authors represent the flux-current relationships with an equivalent star circuit, which requires

all three mutual inductances in Eq. (8.10a) to be equal. This is achieved by modifying (rescaling) the field structure quantities as follows:

$$\lambda_{fm} = \frac{\sqrt{3}}{\sqrt{2}} k \cdot \lambda_f, \quad \textit{and} \quad i_{fm} = \frac{1}{\frac{\sqrt{3}}{\sqrt{2}} k} \cdot i_f \tag{8.14a}$$

$$\textit{with} \qquad k = \frac{M_{af}}{M_{fD}} \tag{8.14b}$$

(identical for λ_D and i_D). Then Eq. (8.10a) becomes

$$\begin{bmatrix} \lambda_d \\ \lambda_{fm} \\ \lambda_{Dm} \end{bmatrix} = \begin{bmatrix} L_d & M_m & M_m \\ M_m & L_{ffm} & M_m \\ M_m & M_m & L_{DDm} \end{bmatrix} \begin{bmatrix} i_d \\ i_{fm} \\ i_{Dm} \end{bmatrix} \tag{8.15a}$$

with

$$M_m = \frac{3}{2} k M_{af}, \qquad L_{ffm} = \frac{3}{2} k^2 L_{ff}, \qquad L_{DDm} = \frac{3}{2} k^2 L_{DD} \tag{8.15b}$$

and

$$R_{fm} = \frac{3}{2} k^2 R_f, \qquad R_{Dm} = \frac{3}{2} k^2 R_D \tag{8.16}$$

Fig. 8.2 shows the equivalent star-circuit for the direct axis, with the speed voltage term and resistances added to make it correct for Eq. (8.9) as well. Modifying the field structure quantities is the same as changing the number of turns in the field structure windings. It does not influence the data conversion, but it is simpler to carry out if the modified form of Eq. (8.15a) is used. The correct turns ratio is then introduced later from the relationship between rated no-load excitation current and rated terminal voltage.

The best data conversion procedure seems to be that of Canay [104]. It uses the four equations which define the open- and short-circuit time constants, as derived in Appendix VI.2, to find R_{fm}, R_{Dm}, L_{ffm} and L_{DDm} ("m" dropped in Appendix VI to simplify the notation). Usually, only one pair of time constants (either T_{d0}', T_{d0}'' or T_d', T_d'') plus X_d', X_d'' are known; in that case, the other pair must first be found from Eq. (8.12). Solving the four equations for the four field structure quantities presupposes that the mutual inductance M_m in Eq. (8.15a) is already known. Its value has traditionally been found from leakage flux calculations. While turns ratios have been

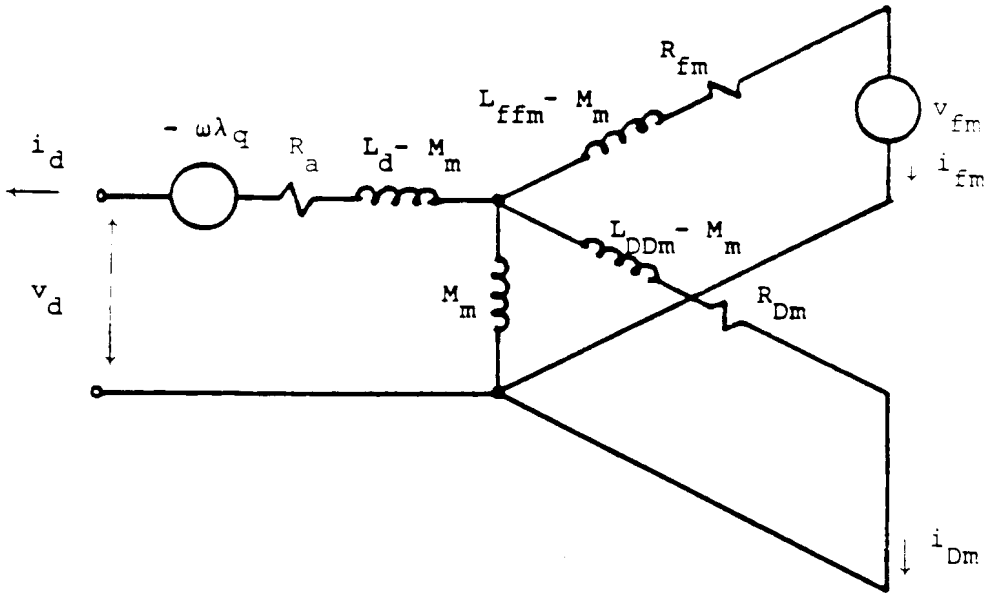

Fig. 8.2 - Equivalent circuit for direct axis with modified field structure quantities

unimportant so far, they must be considered in the definition of leakage flux, since it is the actual flux ϕ, rather than the flux linkage $\lambda = N\phi$ (N = number of turns) which is involved. In defining the leakage flux we must either use actual flux quantities, or flux linkages with turns ratios of 1:1. The leakage flux linkage produced by i_d is then

$$\lambda_{\sigma} = L_d i_d - L_{df} i_d, \qquad \textit{provided} \quad N_d{:}N_f = 1{:}1 \tag{8.17}$$

Let us assume that all field structure quantities are referred to the armature side, which implies $N_a{:}N_f = 1{:}1$ in the original equations (8.4) with phase quantities, with the mutual inductance being M_{af} ($\cos\beta = 1.0$ if magnetic axis of phase 1 armature winding lined up with direct axis). After transforming to d, q, 0- quantities, the mutual inductance in Eq. (8.10a) between d and f changes to $\sqrt{3}/\sqrt{2}\ M_{af}$, which implies that the ratio is now $N_d{:}N_f = \sqrt{3}/\sqrt{2} : 1$. To convert back to a ratio of 1:1, the second row and column in Eq. (8.10a) must be multiplied with $\sqrt{3}/\sqrt{2}$, which changes the mutual inductance to $3/2\ M_{af}$. Then the leakage flux linkage produced by i_d with a 1:1 ratio becomes

$$\lambda_{\sigma} = L_d i_d - \frac{3}{2} M_{af} i_d$$

or for the leakage inductance,

$$L_{\sigma} = L_d - \frac{3}{2} M_{af} \tag{8.18}$$

Unfortunately, this equation is still not enough for finding M_m in the modified matrix of Eq. (8.15a) because of the unknown factor k in Eq. (8.14b). To find k, an additional test quantity must be measured which has not yet been

prescribed in the IEEE or IEC standards. It has therefore been common practice to assume k = 1, which implies $M_{fD} = M_{af}$. With this assumption, the results for armature quantities will be correct, but the amplitude of the fast oscillations in the field current will be incorrect, as pointed out by Canay [104] and others. Fig. 8.3 shows the measured field current after a three-phase short-circuit [104], compared with EMTP simulation results with k = 1, and with the correct value of k. Note that the "d-branch" in the star circuit of Fig. 8.2 is the leakage inductance only if all quantities are referred to the armature

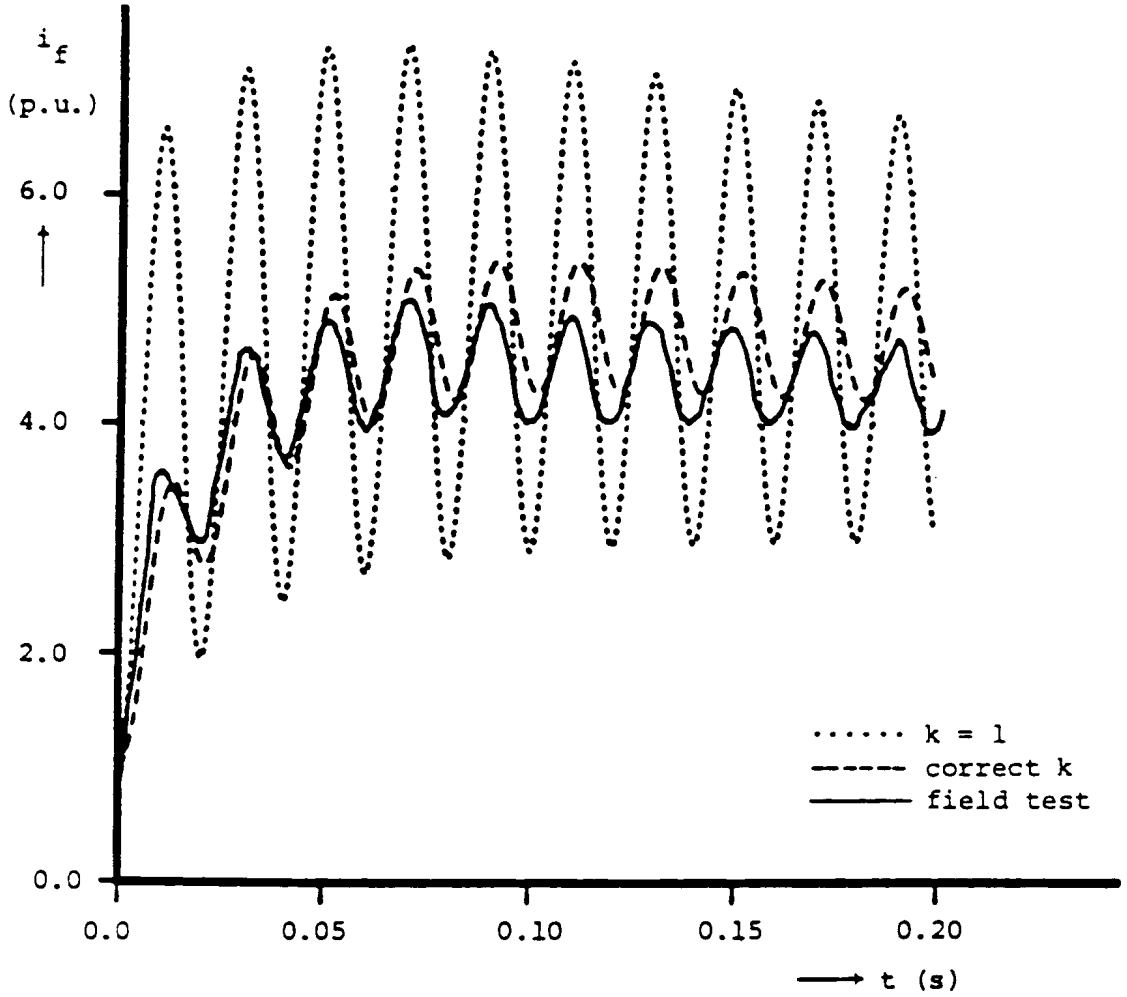

Fig. 8.3 - Field current after three-phase short-circuit [104]. Reprinted by permission of IEE and the author

side and if k = 1. If the factor k is known, then the "d-branch" with field structure quantities referred to the armature becomes Canay's "characteristic inductance"

$$L_c = L_d - \frac{3}{2} k M_{af} \tag{8.19}$$

The data conversion of the modified quantities on the direct axis can now be done as follows: If k is unknown, assume k = 1, find M_m from Eq. (8.18),

$$M_m = L_d - L_{\sigma}$$ (8.20a)

and realize that the fast oscillations in the field current will have a wrong amplitude, but the armature quantities will be correct. If the characteristic inductance is known (which can be calculated from k), find M_m from Eq. (8.19),

$$M_m = L_d - L_c$$ (8.20b)

and the fast oscillations in the field current will be correct. Then use the conversion procedure of Appendix VI.4 to obtain the field structure quantities R_{fm}, R_{Dm}, L_{ffm}, L_{DDm} ("m" dropped in Appendix VI), which will be rescaled according to Eq. (8.14). It is not necessary to undo the rescaling if one is only interested in quantities on the armature side, because scaling of field structure quantities does not influence the armature quantities. If the conversion was done with p.u. quantities, which will usually be the case, then multiply all resistances and inductances with V_{rated}^2/S_{rated} to obtain physical values (V_{rated} = rated line-to-line RMS armature voltage, S_{rated} = rated apparent power) for wye-connected machines, followed by another multiplication with a factor 3 for delta-connected machines.

The data conversion for the quadrature axis quantities is the same as that for the direct axis, except that one does not have to worry about correct amplitudes in the oscillations of the current i_g. This current cannot be measured, because the g-winding is a hypothetical winding which represents eddy or damper bar currents. It is therefore best to use k = 1 and

$$M_{m(quadrature\ axis)} = L_q - L_{\sigma}$$ (8.20c)

on the quadrature axis.

Rather than undo the rescaling of Eq. (8.14) by using t = 1 / ($\sqrt{3}/\sqrt{2}$ k) with the procedure described after Eq. (8.22), it makes more sense to choose a factor t which introduces the correct turns ratio between physical values of the armature and field structure quantities. To find this factor, we must look at the open-circuit terminal voltage produced by the no-load excitation current $i_{f\text{-no load}}$. For open circuit, $i_d = i_q = i_D = 0$, and, in steady-state operation, $d\lambda_q/dt = 0$, which leads to

$$v_q = \omega M_m i_{fm}$$

Since we know that the modified current must be t-times the actual current,

$$i_{fm} = t \cdot i_f$$

and since v_q is equal to $\sqrt{3} \bullet V_{1\text{-RMS}}$ (assuming symmetrical voltages in the three phases), we can find t from

$$t = \frac{\sqrt{3}\, V_{phase}}{\omega M_m i_{f\text{-no load}}}$$ (8.21)

with V_{phase} = rated RMS line-to-ground voltage for wye connection, and line-to-line voltage for delta connection, $i_{f\text{-no load}}$ = rated no-load excitation current which produces rated voltage at the terminal.

Sometimes the no-load excitation current is not known. Then any system of units can be used for the field structure. One possibility is to set t = 1 (field structure quantities referred to the armature side). Another possibility is to say that a field voltage $|v_f| = 1.0$ should produce the rated terminal voltage. Then

$$i_{f\text{-}no\ load} = \frac{|v_f|}{R_f} = \frac{1.0}{t^2 R_{fm}}$$

which, when inserted into Eq. (8.21) gives

$$t = \frac{\omega M_m}{\sqrt{3}\, V_{phase} R_{fm}} \tag{8.22}$$

Once t is known, the inductances are converted by multiplying the second and third row and column of the inductance matrix in Eq. (8.15a) with t, and by multiplying R_{fm} and R_{Dm} with t^2. The quadrature axis inductances and resistances are also multiplied with t or t^2, respectively.

Sometimes, generators are modelled with less than 4 windings on the field structure (D-winding on the direct axis missing, and/or g- or Q-winding on the quadrature axis missing). In such cases, the EMTP still uses the full 7-winding model and simply "disconnects" the unwanted winding by setting its off-diagonal elements in the inductance matrix to zero, and its diagonal element to an arbitrary value of $\omega L = 1\ \Omega$. Its resistance is arbitrarily set to zero. The inductances and resistances of the other windings on the same axis are calculated from Eq. (VI.4) and (VI.5) (Appendix VI), e.g., for a missing g-winding,

$$M_{qg} = 0, \quad M_{gQ} = 0, \quad R_g = 0, \quad \omega L_{gg} = 1$$

and

$$L_{QQ} = \frac{M^2}{L_q - L_q''}, \qquad R_Q = \frac{L_{QQ}}{T_{q0}''}, \qquad where\ M = L_q - L_{\ell}$$

8.3 Basic Equations for Mechanical Part

There are many transient cases where the speed variation of the generator is so small that the mechanical part can be ignored. Simulating short-circuit currents for a few cycles falls into that category. In that case, ω in Eq. (8.6) and in the other equations is constant, and the angular position β of the rotor needed in Eq. (8.7) and (8.9) is simply

$$\beta(t) = \beta(0) + \omega t \tag{8.23}$$

with β and ω being angle and speed on the electrical side.

For other types of studies it may be necessary to take the speed variations into account. The simplest model

for the mechanical part is the single mass representation as used in stability studies,

$$J \frac{d^2\beta}{dt^2} + D \frac{d\beta}{dt} = T_{turbine} - T_{gen} \tag{8.24a}$$

and

$$\frac{d\beta}{dt} = \omega \tag{8.24b}$$

with J = moment of inertia of rotating turbine-generator mass,

β = rotor position,

ω = speed

D = damping coefficient for viscous and windage friction (linear dependence on speed is a crude approximation),

$T_{turbine}$ = torque input to turbine,

T_{gen} = electromagnetic torque of generator.

Eq. (8.24) is valid for quantities referred to the electrical or the mechanical side with the conversion from one to the other being[6]

$$\begin{aligned} J_{e\ell} &= \frac{J_{mech}}{(p/2)^2} \\ \beta_{e\ell} &= \frac{p}{2} \beta_{mech} \\ D_{e\ell} &= \frac{D_{mech}}{(p/2)^2} \\ T_{e\ell} &= \frac{T_{mech}}{p/2} \end{aligned} \tag{8.25}$$

With voltages given in V, and power in W, the unit for the torque T becomes N • m, for the damping coefficient D it becomes N•m / rad/s and for the moment of inertia J it becomes kgm^2 (kg as mass).

Instead of the moment of inertia, the kinetic energy at synchronous speed is often given, which is identical for the mechanical and electrical side,

$$E = \frac{1}{2} J_{mech} \omega_{mech}^2 = \frac{1}{2} J_{e\ell} \omega_{e\ell}^2 \tag{8.26}$$

The inertia constant h (in seconds) is the kinetic energy E (e.g., in kWs) divided by the generator rating S_{rating} (e.g.,

[6]Subscript "mech" is used for the mechanical side, and subscript "eℓ" for the electrical side.

in kVA),

$$h = \frac{E}{S_{rating}} \tag{8.27}$$

The relationship between the inertia constant h and the acceleration time T_a of the turbine-generator is

$$h = \frac{T_a P_{rating}}{2 S_{rating}} \tag{8.28}$$

with P_{rating} = rated power of turbine-generator (e.g., in MW),

S_{rating} = rated apparent power of generator (e.g., in MVA).

A single mass representation is usually adequate for hydro units, where turbine and generator are close together on a stiff shaft. It is not good enough, however, for thermal units, if subsynchronous resonance or similar problems involving torsional vibrations are being studied. In such cases, a number of lumped masses must be represented. Usually 6 to 20 lumped masses provide an adequate model[7]. The model in the EMTP allows any number of lumped masses $n \geq 1$, and automatically includes the special case of $n = 1$ in Eq. (8.24). Each major element (generator, high pressure turbine, etc.) is considered to be a rigid mass connected to adjacent elements by massless springs. Fig. 8.4 shows a typical 7-mass model.

The shaft/rotor system is assumed to be linear, which is reasonable for the small amplitudes of typical torsional vibrations. The n spring-connected rotating masses are then described by the rotational form of Newton's second law,

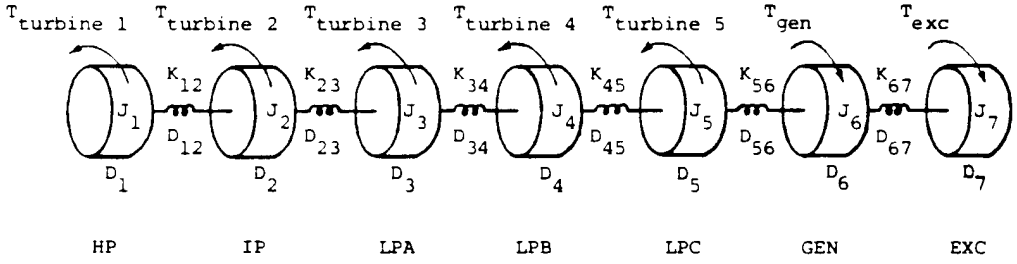

Fig. 8.4 - Mechanical part of a steam turbine generator with 7 masses (HP = high pressure turbine, IP = intermediate pressure turbine, LPA, LPB, LPC = low pressure turbine stages A, B, C, GEN = generator, EXC = exciter)

$$[J]\frac{d^2}{dt^2}[\theta] + [D]\frac{d}{dt}[\theta] + [K][\theta] = [T_{turbine}] - [T_{gen/exc}] \tag{8.29a}$$

and

[7]There are studies where the lumped mass representation is no longer adequate, and where continuum models must be used.

$$\left[\frac{d\theta}{dt}\right] = [\omega] \tag{8.29b}$$

where

[J] = diagonal matrix of moments of inertia (J_1,...J_7 in Fig. 8.4),

[θ] = vector of angular positions (θ_1,...θ_7 in Fig. 8.4, with $\theta_6 = \beta$),

[ω] = vector of speeds,

[D] = tridiagonal matrix of damping coefficients,

[K] = tridiagonal matrix of stiffness coefficients,

$[T_{turbine}]$ = vector of torques applied to the turbine stages ($T_{turbine6} = 0$ and $T_{turbine7} = 0$ in Fig. 8.4),

$[T_{gen/exc}]$ = vector of electromagnetic torques of generator and exciter (components 1 to 5 = 0 in Fig. 8.4).

The moments of inertia and the stiffness coefficients are normally available from design data. The spring action of the shaft section between masses i - 1 and i creates a torque which is proportional to the angle twist θ_{i-1}-θ_i. The proportionality factor is the stiffness coefficient or spring constant $K_{i-1,i}$. This spring action torque acts in opposite directions on masses i - 1 and i,

$$T_{spring,i-1} = -T_{spring,i} = K_{i-1,i}\left(\theta_{i-1}-\theta_i\right) \tag{8.30}$$

If these torques are included in Eq. (8.29), they create the term [K][θ]. From Eq. (8.30) it can be seen that [K] has the following form

$$[K] = \begin{bmatrix} K_{12} & -K_{12} & & & \\ -K_{12} & K_{12}+K_{23} & -K_{23} & & \\ & -K_{23} & K_{23}+K_{34} & -K_{34} & \\ . & . & . & . & . \\ & & & -K_{n-1,n} & K_{n-1,n} \end{bmatrix}$$

Two damping effects are included with the damping coefficients, namely the self-damping D_i of mass i (mostly friction between the turbine blades and steam), and the damping $D_{i-1,i}$ created in the shaft when the shaft between masses i - 1 and i is twisted with the speed ω_i - ω_{i-1}. The damping torque acting on mass i is therefore

$$T_{damping,i} = D_i\frac{d\theta_i}{dt} + D_{i-1,i}\left(\frac{d\theta_i}{dt} - \frac{d\theta_{i-1}}{dt}\right) + D_{i,i+1}\left(\frac{d\theta_i}{dt} - \frac{d\theta_{i+1}}{dt}\right) \tag{8.31}$$

From Eq. (8.31) it can be seen that [D] has the same structure as [K], except that the diagonal element is now $D_{i-1,i}$ + D_i + $D_{i,i+1}$,

$$[D] = \begin{bmatrix} D_1 + D_{12} & -D_{12} & & & \\ -D_{12} & D_{12} + D_2 + D_{23} & -D_{23} & & \\ . & . & . & . & . \\ & & & -D_{n-1,n} & D_{n-1,n} + D_n \end{bmatrix}$$

It is very difficult to obtain realistic values for these damping coefficients. Fortunately, they have very little influence on the peak torque values during transient disturbances. However, for estimating the low cycle fatigue one must consider the damping terms, which, unfortunately until now, have often been derived from unsuitable models [107]. The damping of torsional oscillations is measured by observing the rate of decay when the shaft system is excited at one of its natural frequencies (modes). It is difficult to convert these modal damping coefficients into the diagonal and off-diagonal elements of [D].

For the vector of turbine torques it is best to assume that the turbine power $P_{turbine} = \omega \bullet T_{turbine}$ remains constant. This implies that the torque decreases with an increase in speed, which is more reasonable than constant torque because if the turbine were to reach the same speed as the steam (or water) jet the torque on the blades would obviously drop to zero. It is possible to include the effects of the speed governor through TACS modelling, but usually the time span of transient simulations is so short that the governor effects will normally not show up.

The vector of electromagnetic torques and the rotor position of the generator provide the link between the equations of the mechanical and electrical part, with

$$\theta_{mech-gen} \cdot \frac{p}{2} = \beta_{elec} \tag{8.32a}$$

$$T_{mech-gen} = \frac{p}{2}(\lambda_d i_q - \lambda_q i_d) \tag{8.32b}$$

$$T_{mech-exc} = \frac{-v_f i_f + i_f^2 R_{exc}}{\omega_{mech}} \tag{8.32c}$$

where it is assumed that (Eq. 8.29) is written for the mechanical side. If it is written for the electrical side, then the conversion of Eq. (8.25) must be used. The term $i_f^2 R_{exc}$ in Eq. (8.32c) represents the losses incurred in the exciter machine; the negative sign for v_f comes from the source convention of Eq. (8.1). If there is no exciter machine, as in the case of rectifier excitation systems, then mass no. 7 in Fig. 8.4 would obviously be deleted, and Eq. (8.32c) would not be needed. $T_{mech-exc}$ is not in the BPA EMTP.

8.4 Steady-State Representation and Initial Conditions

Transient studies with detailed turbine-generator models practically always start from power frequency

steady-state conditions. The EMTP goes therefore automatically into an ac steady-state solution whenever the data file contains turbine-generator models.

In some versions of the BPA EMTP, the machine is represented as a symmetrical voltage source at its terminals. This approach is only correct if the generator feeds into a balanced network. In that case, the generator currents are purely positive sequence. In an unbalanced network, there are negative and zero sequence currents, which would see the generator as a short-circuit. This is incorrect, because generators do have nonzero negative and zero sequence impedances Z_{neg} and Z_{zero}. In the M39 version of the BPA EMTP, the user can specify unsymmetrical voltage sources at the terminals. This is still not good enough, however, unless the user adjusts the negative and zero sequence components of the terminal voltage iteratively until $V_{neg} = -Z_{neg}I_{neg}$ and $V_{zero} = -Z_{zero}I_{zero}$, with I_{neg}, I_{zero} being the currents from the steady-state network solution. The UBC EMTP does include negative and zero sequence impedances correctly, as explained next.

The negative sequence impedance can be calculated as part of the data conversion. Its imaginary part is very close to

$$X_{neg} \approx \frac{X_{d''} + X_{q''}}{2} \tag{8.33}$$

and this value can be used without too much error if the negative sequence impedance is needed for preliminary calculations. The real part R_{neg} is larger than the armature resistance R_a because of double-frequency circulating currents in the field structure circuits; its value is difficult to guess, and is therefore best taken from the data conversion. For calculations internal to the UBC EMTP, the correct values from the data conversion are always used. The zero sequence impedance $Z_{zero} = R_a + kX_{zero}$ is part of the input data, but its value becomes immaterial if the generator step-up transformer is delta-connected on the generator side and if the disturbance occurs on the line side.

The positive sequence representation can be a voltage source behind any impedance, as long as it produces the desired values for the terminal voltage V_{pos} and the current I_{pos}. Knowing only V_{pos} may require a preliminary steady-state solution with a voltage source V_{pos} at the terminal, to find I_{pos}. Then the value needed for the voltage source behind the impedance is

$$V_{source} = V_{pos} + Z I_{pos}$$

Any value can be chosen for Z, but $Z = Z_{neg}$ simplifies programming for the following reason: The EMTP solves the network in phase quantities, and assumes that all phase impedance matrices are symmetric. Only $Z = Z_{neg}$ will produce a symmetric phase impedance matrix, however. Changing the program to handle unsymmetric matrices just for generators would have required a substantial amount of re-programming.

The generator positive sequence representation is then a voltage source behind Z_{neg} while the negative and zero sequence representations are passive impedances Z_{neg} and Z_{zero}, respectively (or zero voltage sources or short-circuits behind Z_{neg} and Z_{zero}). Converted to phase quantities, these 3 single-phase sequence representations become

a three-phase symmetrical voltage source (E_1", E_2", E_3") behind a 3 x 3 impedance matrix, as shown in Fig. 8.5(a), with

$$[Z] = \begin{bmatrix} Z_s & Z_m & Z_m \\ Z_m & Z_s & Z_m \\ Z_m & Z_m & Z_s \end{bmatrix} \tag{8.34}$$

$$\textit{where} \qquad Z_s = \frac{1}{3}(Z_{zero} + 2\,Z_{neg}) \;, \qquad Z_m = \frac{1}{3}(Z_{zero} - Z_{neg})$$

To be able to handle any type of connection, including delta and impedance-grounded or ungrounded wye connections, the voltage sources behind [Z] are converted into current sources in parallel with [Z], as indicated in Fig. 8.5(b), with

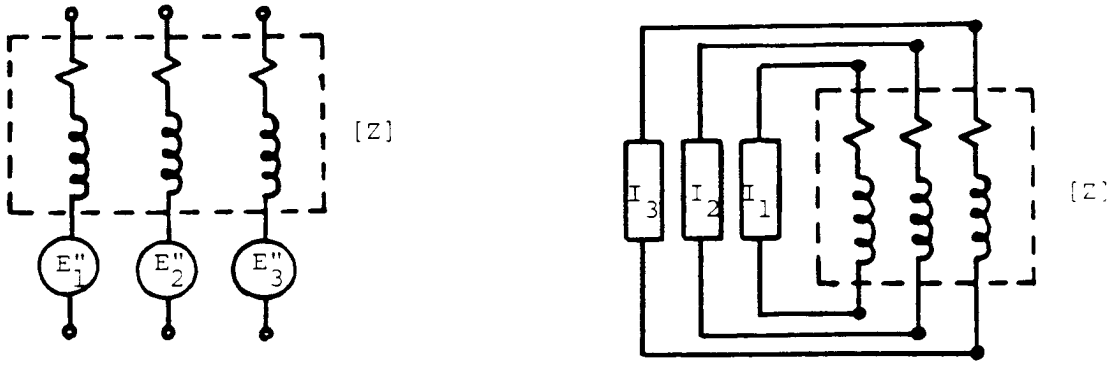

(a) Thevenin equivalent circuit (b) Norton equivalent circuit

Fig. 8.5 - Turbine-generator representation for steady-state solution

$$\begin{bmatrix} I_1 \\ I_2 \\ I_3 \end{bmatrix} = [Z]^{-1} \begin{bmatrix} E_1'' \\ E_2'' \\ E_3'' \end{bmatrix} \tag{8.35}$$

This is done because the EMTP could not handle voltage sources between nodes until recently and even after such voltage sources are allowed now, this Norton equivalent circuit is at least as efficient. For armature winding 1, the internal voltage source is

$$E_1'' = V_{pos} + Z_{neg} I_{pos} \tag{8.36}$$

with V_{pos}, I_{pos} being the unnormalized positive sequence values. Unnormalized values are a more convenient input form for the user, because with the unnormalized transformation of Eq. (8.38) the positive sequence values are identical with the phase values V_1 and I_1 for armature winding 1 for balanced network conditions. For armature windings 2 and 3, the internal voltages are

$$E_2'' = a^2 E_1'' \qquad and \qquad E_3'' = a E_1'' \tag{8.37}$$

$a = e^{j120^\circ}$).

In the UBC EMTP, either V_{pos} and I_{pos} can be specified as input data, in which case E_1" is calculated from Eq. (8.36), or E_1" can be specified directly. Specifying E_1" is not as unusual as it may seem, because short-circuit programs use essentially the same generator representation (E" behind X_d"). If users want to specify active and reactive power at the terminals, or active power and voltage magnitude, then the load flow option described in Section 12.2 can be invoked, which will automatically produce the required V_{pos} and I_{pos}.

The UBC EMTP connects the generator model of Fig. 8.5(b) to the network for the steady-state solution, which will produce the terminal voltages and currents at fundamental frequency. For unbalanced network conditions, this solution method is not quite correct because it ignores all harmonics in the armature windings and in the network. Experience has shown, however, that such an approximate initialization is accurate enough for practical purposes. Fig. 8.6 shows simulation results for a generator feeding into a highly unbalanced load resistance (R_A = 1.0 Ω, R_B = 1.0 Ω, R_C = 0.05 Ω), with an initialization procedure which ignores the harmonics on the armature side, and considers only the second harmonics on the field structure side, as discussed in Section 8.4.2. The final steady state is practically present from the start. The mechanical part is totally ignored in the steady-state solution, because it is assumed that the generator runs at synchronous speed. Again, for unbalanced conditions this is not quite correct

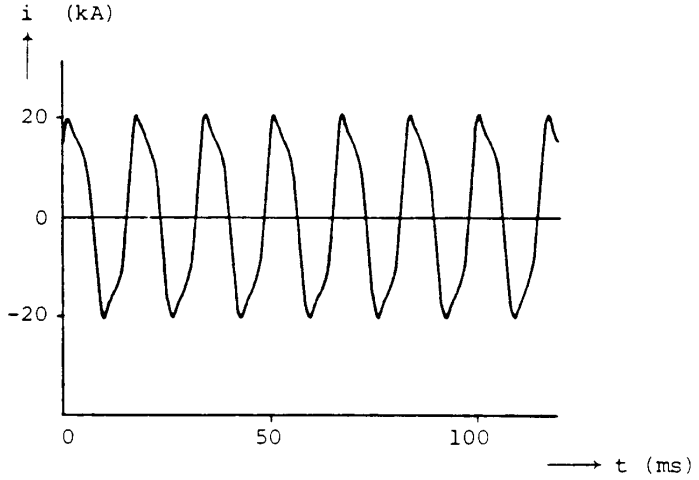

Fig. 8.6 - Steady-state behavior of generator with highly unbalanced load

because, in that case, the constant electromagnetic torque has oscillations superimposed on it which produce torsional

vibrations whose effects are ignored.

After the steady-state solution at fundamental frequency has been obtained, the terminal voltages and currents are converted to unnormalized symmetrical components to initialize the machine variables:

$$\begin{bmatrix} V_{zero} \\ V_{pos} \\ V_{neg} \end{bmatrix} = \frac{1}{3}\begin{bmatrix} 1 & 1 & 1 \\ 1 & a & a^2 \\ 1 & a^2 & a \end{bmatrix}\begin{bmatrix} V_1 \\ V_2 \\ V_3 \end{bmatrix}, \quad \textit{identical for currents} \tag{8.38}$$

($a = e^{j120^\circ}$). The inverse transformation is

$$\begin{bmatrix} V_1 \\ V_2 \\ V_3 \end{bmatrix} = \begin{bmatrix} 1 & 1 & 1 \\ 1 & a^2 & a \\ 1 & a & a^2 \end{bmatrix}\begin{bmatrix} V_{zero} \\ V_{pos} \\ V_{neg} \end{bmatrix}, \quad \textit{identical for currents} \tag{8.39}$$

8.4.1 Initialization with Positive Sequence Values

If the positive sequence voltage is obtained as a peak (not RMS) phasor value $|V_{pos}|e^{j\gamma pos}$, then from Eq. (8.39),

$$v_1(t) = |V_{pos}|\cos(\omega t + \gamma_{pos})$$

$$v_2(t) = |V_{pos}|\cos(\omega t + \gamma_{pos} - 120^\circ) \tag{8.40}$$

$$v_3(t) = |V_{pos}|\cos(\omega t + \gamma_{pos} + 120^\circ)$$

Inserting these voltages into the transformation of Eq. (8.7) produces

$$v_{d\text{-}pos}(t) = \frac{\sqrt{3}}{\sqrt{2}}|V_{pos}|\sin(\gamma_{pos} - \delta)$$

$$v_{q\text{-}pos}(t) = \frac{\sqrt{3}}{\sqrt{2}}|V_{pos}|\cos(\gamma_{pos} - \delta) \tag{8.41}$$

where δ is the angle between the position of the quadrature axis and the real axis for phasor representations (Fig. 8.7). This angle is related to the rotor position $\beta_{e\ell}$ on the electrical side by

$$\beta_{e\ell} = \omega t + \delta + \frac{\pi}{2} \tag{8.42}$$

The positive sequence values v_d and v_q in Eq. (8.41) are dc quantities and hence do not change as a function of time; the argument (t) can therefore be dropped. From Eq. (8.41) it is evident that v_d and v_q can be combined into a complex expression

$$v_{q\text{-}pos} + j v_{d\text{-}pos} = \frac{\sqrt{3}}{\sqrt{2}} V_{pos}\, e^{-j\delta} \tag{8.43}$$

with V_{pos} being the complex quantity $|V_{pos}|e^{j\gamma pos}$. While V_{pos} is a phasor of frequency ω in the network solution reference frame, $V_{pos}\, e^{-j\delta}$ in Eq. (8.43) becomes a dc quantity in the d, q-axes reference frame. Similarly,

$$i_{q\text{-}pos} + j i_{d\text{-}pos} = \frac{\sqrt{3}}{\sqrt{2}} I_{pos}\, e^{-j\delta} \tag{8.44}$$

with I_{pos} being the complex current $|I_{pos}|e^{j\alpha pos}$ with respect to the real axis. With V_{pos} and I_{pos}

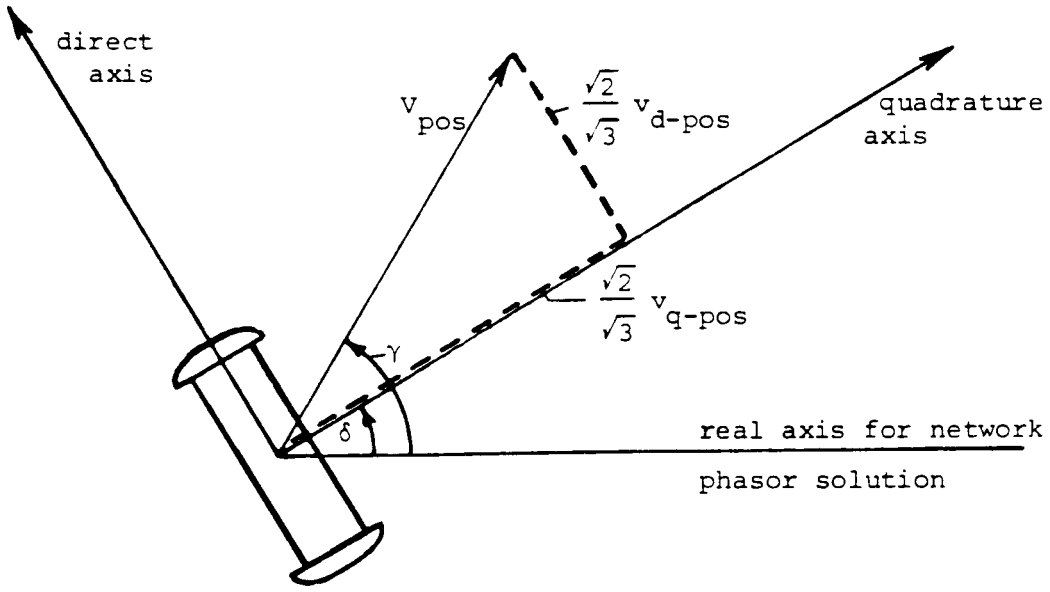

Fig. 8.7 - Definition of δ

known, we still need the angle δ to find the d, q-values. To calculate δ, use Eq. (8.9) and Eq. (8.10), with $i_D = i_g = i_Q = 0$, as well as $d\lambda_d/dt = 0$ and $d\lambda_q/dt = 0$ (no currents in damper windings and all d, q-quantities constant in symmetrical operation with positive sequence values only),

$$v_{d\text{-}pos} = -R_a i_{d\text{-}pos} - \omega L_q i_{q\text{-}pos} \tag{8.45a}$$

$$v_{q\text{-}pos} = -R_a i_{q\text{-}pos} + \omega L_d i_{d\text{-}pos} + \omega M_{df} i_{f\text{-}pos} \tag{8.45b}$$

Eq. (8.45a) and (8.45b) can be rewritten as a complex equation relative to the quadrature axis

$$v_{q\text{-}pos} + jv_{d\text{-}pos} = -(R_a + j\omega L_q)(i_{q\text{-}pos} + ji_{d\text{-}pos}) + E_{q\text{-}pos} \tag{8.45c}$$

where $E_{q\text{-}pos}$ is a quantity whose position on the quadrature axis is important, but whose magnitude

$$E_{q\text{-}pos} = (\omega L_d - \omega L_q)\, i_{d\text{-}pos} + \omega M_{df} i_{f\text{-}pos}$$

is immaterial here. By inserting Eq. (8.43) and Eq. (8.44) into Eq. (8.45c), and by multiplying with $(\sqrt{2}/\sqrt{3})e^{j\delta}$, all dc quantities become phasors in the network solution reference frame again. The angle δ is then obtained from the phasor equation

$$\frac{\sqrt{2}}{\sqrt{3}} \Delta v_{q\text{-}pos}\, e^{j\delta} = V_{pos} + (R_a + j\omega L_q)\, I_{pos} \tag{8.46}$$

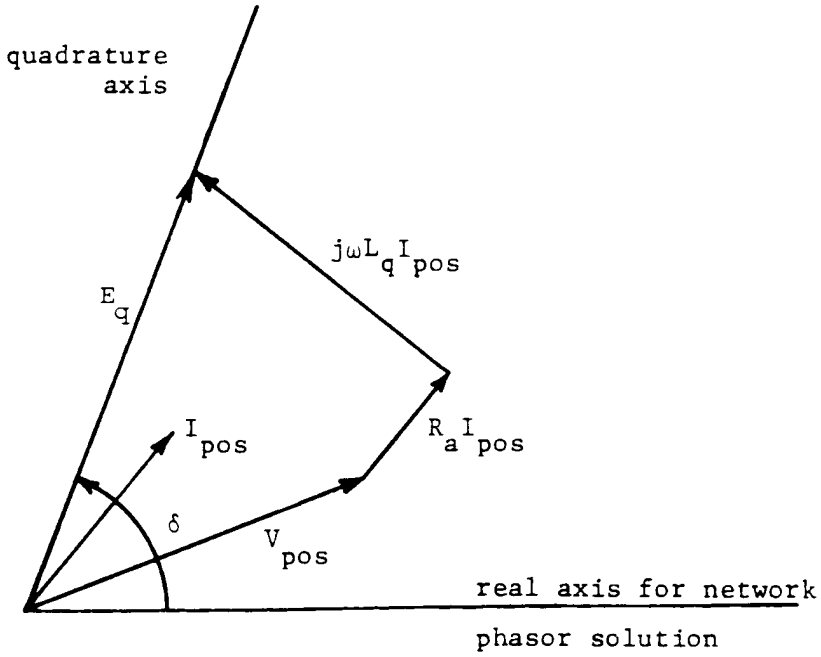

Fig. 8.8 - Calculation of angle δ

With δ known, the initial values $v_{d\text{-}pos}(0)$, $v_{q\text{-}pos}(0)$, $i_{d\text{-}pos}(0)$, $i_{q\text{-}pos}(0)$ are found from Eq. (8.43) and (8.44). As mentioned before, the remaining currents i_D, i_g, i_Q are zero from the positive sequence effects, except for i_f, whose initial value is calculated from Eq. (8.45b),

$$i_{f\text{-}pos}(0) = \frac{v_{q\text{-}pos}(0) + R_a i_{q\text{-}pos}(0) - \omega L_d i_{d\text{-}pos}(0)}{\omega M_{df}} \tag{8.47}$$

$i_{f\text{-}pos}(0)$ is used to initialize v_f

$$v_{f\text{-}pos}(0) = -R_f i_{f\text{-}pos}(0) \tag{8.48}$$

The initial value of the torque produced by the positive sequence quantities is needed in the mechanical part. It is calculated from the fluxes $\lambda_{d\text{-}pos}(0) = L_d i_{d\text{-}pos}(0) + M_{df} i_{f\text{-}pos}(0)$ and $\lambda_{q\text{-}pos}(0) = L_q i_{q\text{-}pos}(0)$ as

$$T_{gen\text{-}pos}(0) = \lambda_{d\text{-}pos}(0)\, i_{q\text{-}pos} - \lambda_{q\text{-}pos}(0)\, i_{d\text{-}pos}(0) \tag{8.49}$$

The initial positive sequence torque can also be calculated from energy balance considerations (ωT = power delivered to the network + losses in the armature windings),

$$\omega T_{gen\text{-}pos}(0) = \frac{3}{2} Re\{I_{pos} V_{pos}^{*}\} + \frac{3}{2} |I_{pos}|^2 R_a \tag{8.50}$$

(division by 2 because the phasors are peak values).

8.4.2 Initialization with Negative Sequence Values[8]

If the network is balanced in steady state, then there are no negative sequence values. This part of the initialization can therefore be skipped if the negative sequence (peak) phasor current

$$I_{neg} = |I_{neg}|\, e^{j\alpha_{neg}} \tag{8.51}$$

obtained from the steady-state solution is negligibly small.

Negative sequence currents in the armature windings create a magnetic field which rotates backwards at a relative speed of 2ω with respect to the field structure. Second harmonic currents are therefore induced in all windings on the field structure, which the EMTP takes into account in the initialization. These second harmonic currents induce third harmonics in the armature windings, which in turn produce fourth harmonics in the field structure windings, etc. Fortunately, these higher harmonics decrease rapidly in magnitude. They are therefore ignored. Calculating the field structure harmonics or order higher than 2 could be done fairly easily, but the calculation of the armature harmonics of order 3 and higher would involve solutions of the complete network at these higher frequencies. While the network solutions for harmonics may be added to the EMTP someday, this addition does not appear to be justified for this particular purpose.

First, the negative sequence current must be defined on the direct and quadrature axis. By starting with the negative sequence currents in the three armature windings,

$$\begin{aligned} i_1(t) &= |I_{neg}| \cos(\omega t + \alpha_{neg}) \\ i_2(t) &= |I_{neg}| \cos(\omega t + \alpha_{neg} + 120°) \\ i_3(t) &= |I_{neg}| \cos(\omega t + \alpha_{neg} - 120°) \end{aligned} \tag{8.52}$$

[8]The negative sequence currents in the BPA EMTP can be incorrect (see beginning of Section 8.4).

these d, q-axes values are obtained through the transformation (8.7),

$$i_{d-neg}(t) = -\frac{\sqrt{3}}{\sqrt{2}} |I_{neg}| \sin(\alpha_{neg} + \delta + 2\omega t)$$
$$i_{q-neg}(t) = \frac{\sqrt{3}}{\sqrt{2}} |I_{neg}| \cos(\alpha_{neg} + \delta + 2\omega t) \tag{8.53}$$

While the positive sequence d, q-axes currents are dc quantities, the negative sequence d, q-axes currents are second harmonics. This is important to keep in mind when we represent them with a phasor of frequency 2ω,

$$I_{dq-neg} = \frac{\sqrt{3}}{\sqrt{2}} I_{neg} e^{j\delta} \tag{8.54}$$

with the understanding that

$$i_{d-neg}(t) = -Im\{I_{dq-neg} e^{j2\omega t}\}$$
$$i_{q-neg}(t) = Re\{I_{dq-neg} e^{j2\omega t}\} \tag{8.55}$$

For the initialization of i_d and i_q, the negative sequence values at t = 0 from Eq. (8.55) must be added to the respective positive sequence values from Eq. (8.44) to obtain the total initial values $i_d(0)$ and $i_q(0)$. The negative sequence d, q-axes voltages are not needed in the initialization, but they could be obtained analogously to the currents.

The second harmonic currents in the field structure windings are found by using the d, q-axes phasor current of frequency 2ω as the forcing function. The procedure is outlined for the direct axis; it is analogous for the quadrature axis. From Eq. (8.1),

$$v_{f-neg} = -R_f i_{f-neg} - \frac{d}{dt}(M_{df} i_{d-neg} + L_{ff} i_{f-neg} + M_{fD} i_{D-neg})$$
$$v_{D-neg} = -R_D i_{D-neg} - \frac{d}{dt}(M_{dD} i_{d-neg} + M_{fD} i_{f-neg} + L_{DD} i_{D-neg}) \tag{8.56}$$

The voltages on the left-hand side are zero because the damper winding is always shorted, and the dc voltage source supplying the field winding is seen as a short-circuit by second harmonic currents. With zero voltages, and knowing that all currents are second harmonics, Eq. (8.56) can be rewritten as two phasor equations

$$\begin{bmatrix} R_f + j2\omega L_{ff} & j2\omega M_{fD} \\ j2\omega M_{fD} & R_D + j2\omega L_{DD} \end{bmatrix} \begin{bmatrix} I_{f-neg} \\ I_{D-neg} \end{bmatrix} = - \begin{bmatrix} j2\omega M_{df} \\ j2\omega M_{dD} \end{bmatrix} I_{dq-neg} \tag{8.57}$$

which are solved for the two phasors $I_{f\text{-}neg}$, $I_{D\text{-}neg}$. Their initial values are found on the basis of Eq. (8.55) as

$$i_{f-neg}(0) = - Im\{I_{f-neg}\}$$

$$i_{D-neg}(0) = - Im\{I_{D-neg}\} \tag{8.58}$$

The value $i_{f\text{-}neg}(0)$ is then added to $i_{f\text{-}pos}(0)$ from Eq. (8.47) for the total initial field current, whereas $i_{D\text{-}neg}(0)$ is already the value of the total damper current.

The phasor currents $I_{g\text{-}neg}$ and $I_{Q\text{-}neg}$ for the quadrature axis are obtained analogous to Eq. (8.58), by replacing subscripts f and D with g and Q. Their initial values on the basis of Eq. (8.55) are then

$$i_{g-neg}(0) = Re\{I_{g-neg}\}$$

$$I_{Q-neg}(0) = Re\{I_{Q-neg}\} \tag{8.59}$$

which are the total initial values since the respective positive sequence values are zero.

The negative sequence phenomena produce torques which influence the initialization of the mechanical part. Recall that the electromagnetic torque on the electrical side is $\lambda_d i_q - \lambda_q i_d$. With both fluxes and currents consisting of positive and negative sequence parts, the total torque can be expressed as the sum of three terms,

$$T_{gen} = T_{gen-pos} + T_{gen-neg} + T_{gen-pos/neg} \tag{8.60}$$

The positive sequence torque was already defined in Eq. (8.49), and the negative sequence torque is

$$T_{gen-neg} = \lambda_{d-neg} i_{q-neg} - \lambda_{q-neg} i_{d-neg} \tag{8.61}$$

The third term

$$T_{gen-pos/neg} = \lambda_{d-pos} i_{q-neg} + \lambda_{d-neg} i_{q-pos} - \lambda_{q-pos} i_{d-neg} - \lambda_{q-neg} i_{d-pos} \tag{8.62}$$

is an oscillating torque produced by the interaction between positive and negative sequence quantities, with an average value of zero. That it is purely oscillatory can easily be seen since all positive sequence values in Eq. (8.62) are constant, and all negative sequence values oscillate at a frequency of 2ω. This and other oscillating terms are ignored in the initialization of the mechanical part, where torsional vibrations are not taken into account.

The negative sequence torque of Eq. (8.61) consists of a constant part, which must be included in the initialization of the mechanical part, and of an oscillating part with frequency 4ω which is ignored. To find the constant part, the fluxes are first calculated as phasors,

$$\Lambda_{d-neg} = L_d I_{dq-neg} + M_{df} I_{f-neg} + M_{dD} I_{D-neg} \tag{8.63a}$$

$$\Lambda_{q-neg} = L_q I_{dq-neg} + M_{qg} I_{g-neg} + M_{qQ} I_{Q-neg} \tag{8.63b}$$

With the definition of Eq. (8.55) for the instantaneous values of currents and fluxes, and after some manipulations of the equations, it can be shown that the constant part is

$$T_{gen-neg-constant} = Re\{\Lambda_{average}\} Im\{I_{dq-neg}\} - Im\{\Lambda_{average}\} Re\{I_{dq-neg}\} \tag{8.64a}$$

with

$$\Lambda_{average} = \frac{1}{2}(\Lambda_{d-neg} + \Lambda_{q-neg}) \tag{8.64b}$$

The oscillatory part is not needed, but could be calculated from

$$T_{gen-neg-oscillatory} = Im\left\{\frac{\Lambda_{q-neg} - \Lambda_{d-neg}}{2} I_{dq-neg}\, e^{j4\omega t}\right\} \tag{8.65}$$

Identical values for the constant part are obtained from energy balance considerations (ωT = power delivered to network + losses in all windings),

$$\omega T_{gen-neg-constant} = \frac{1}{2}\{-3|I_{neg}|^2(R_{neg} - R_a) + |I_{f-neg}|^2 R_f + |I_{g-neg}|^2 R_g + |I_{D-neg}|^2 R_D + |I_{Q-neg}|^2 R_Q\} \tag{8.66}$$

Because 3rd and higher order harmonics are ignored in the armature windings, and 4th and higher order harmonics are ignored in the windings on the field structure, the initial torque values are not exact. They are good approximations, however, as can be seen from Table 8.1. This table compares the values obtained from the initialization equations with the values obtained from a transient simulation (Fig. 8.9), for the severely unbalanced case described in Fig. 8.6. The constant torque from the initialization procedure is almost identical with the average torque of the transient simulation (difference 1.6%). Fig. 8.9 further shows that the initial torque from Eq. (8.73) can be quite different from the average torque. Table 8.1 also compares the values for the 2nd and 4th harmonics (not needed in the initialization, though). The values for the 2nd harmonic agree quite well, but not the values for the smaller 4th harmonic. This is to be expected, because the 4th harmonic torque is influenced by 3rd harmonic currents in the armature windings, which are ignored in this initialization procedure. The average value in Fig. 8.9 lies not exactly halfway between the maximum and minimum values because the 4th harmonic is phase-shifted with respect to the second harmonic.

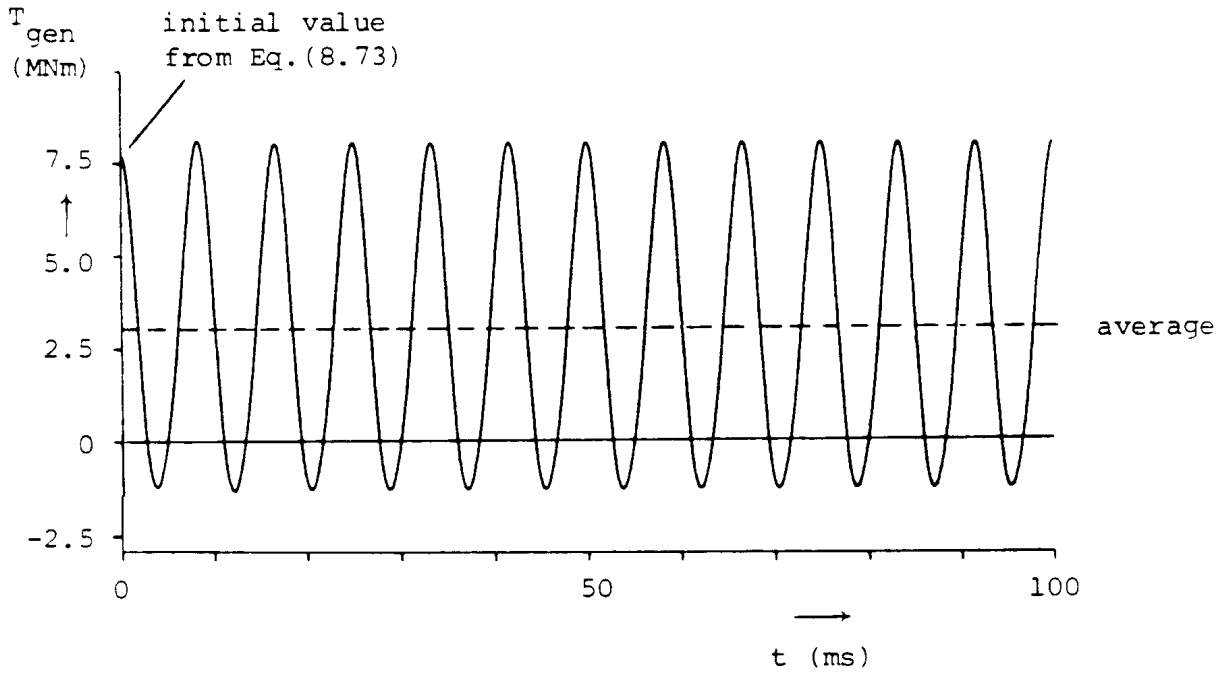

Fig. 8.9 - Torque obtained with transient simulation for case described in Fig. 8.6

Table 8.1 - Electromagnetic torque for test case of Fig. 8.6 ($\Delta t = 46.2963\ \mu s$)

Torque Component	From Equations (MNm)	From Fourier Analysis Between 80 ms and 100 ms (MNm)	Relative Error (%)
average	pos = 2.953 from (8.49) or (8.50) neg = 0.017 from (8.64) or (8.66) sum = 2.970	3.019	1.62
2nd harmonic	4.673	4.634	0.84
4th harmonic	0.262	0.517	49.32

8.4.3 Initialization with Zero Sequence Values[9]

The initial zero sequence values are easy to obtain, either from the d, q, 0-transformation of Eq. (8.7), or from the symmetrical component transformation of Eq. (8.38). Physically, both are the same quantities, except that

[9]The zero sequence currents in the BPA EMTP can be incorrect (see beginning of Section 8.4).

the d, q, 0-transformation is normalized and the symmetrical component transformation chosen in Eq. (8.38) is not. Since the d, q, 0-quantities are normalized,

$$i_0(0) = \frac{1}{\sqrt{3}} (i_a(0) + i_b(0) + i_c(0)) \tag{8.67a}$$

or

$$i_0(0) = \sqrt{3}\, Re\{I_{zero}\} \tag{8.67b}$$

The zero sequence quantities do not produce any torque, and therefore do not influence the initialization of the mechanical part.

8.4.4 Initialization of the Mechanical Part[10]

The links between the electrical and the mechanical part are the angle $\beta_{el}(0)$ from Eq. (8.42), which is converted to the mechanical side with Eq. (8.25), and the electromagnetic torques T_{gen} and T_{exc} from Eq. (8.32). For the generator torque, the constant part is

$$T_{gen-constant} = T_{gen-pos}(0) + T_{gen-neg-constant} \tag{8.68}$$

on the electrical side, which is converted with Eq. (8.25) to the mechanical side. Since torsional vibrations coming from the oscillating torques of Eq. (8.62) and Eq. (8.65) in unbalanced cases are ignored in the steady-state initializations, the oscillating term is left off in Eq. (8.68). For the exciter torque, the oscillating terms are ignored as well. Then,

$$\omega T_{exc-constant} = -v_{f-pos}(0)\, i_{f-pos}(0) + \frac{1}{2} |I_{f-neg}|^2 R_{exc} \tag{8.69}$$

with $I_{f\text{-}neg}$ from Eq. (8.57).

Without torsional vibrations, the speeds of all turbine-generator masses are one and the same, and the acceleration of each mass is zero. Then Eq. (8.29) simplifies to

$$[K][\theta] = [T_{turbine}] - [T_{gen/exc}] - \omega [D_{self}] \tag{8.70}$$

with ω being the synchronous angular speed and $[D_{self}]$ being the diagonal matrix of self-damping terms D_i. The sum of the turbine torques must, of course, equal the sum of the electromagnetic and speed self-damping torques, so that there is zero accelerating torque initially,

$$\sum T_{turbine-i} = T_{gen-constant} + T_{exc-constant} + \omega \sum D_i \tag{8.71}$$

---

[10]The initial angles in the BPA EMTP can be incorrect in unbalanced cases, because the negative sequence torques are not included in Eq. (8.68) and (8.69). If Table 8.1 is typical, these torques are very small, however.

Eq. (8.71) is used to find the sum of the turbine torques first, and then to apportion the total to the individual stages from the percentage numbers to be supplied in the input (e.g., 30% of torque in high pressure stage, 26% in intermediate pressure stage, etc.). The right-hand side of Eq. (8.70) is then known, as well as the angle of the generator mass from Eq. (8.32a). [K] is singular. Assume the generator to be mass no. k (with θ_k known); then the remaining initial angles may be found in 2 ways:

(1) Multiply the diagonal element K_{kk} with an arbitrary large number (e.g., 10^{30}), and reset the k-th right-hand side value to this number times θ_k. This will, in effect, change the k-th equation to variable θ_k = specified value of θ_k. Then solve the system of linear equations (8.70), preferably with a subroutine for tri-diagonal matrices (required in the time-step loop anyhow).

(2) Starting to the left of generator mass k, find the angles of the lower-numbered masses recursively from

$$\theta_{i-1} = \theta_i + \frac{\sum_{1}^{i-1} RHS}{K_{i-1,\,i}}, \quad i = k,\ldots 1 \tag{8.72a}$$

(RHS = right-hand side terms of Eq. (8.70)), and starting to the right of generator mass k, find the angles of the higher-numbered masses recursively from

$$\theta_{i+1} = \theta_i + \frac{\sum_{i+1}^{n} RHS}{K_{i,\,i+1}}, \quad i = k,\ldots n \tag{8.72b}$$

These recursive equations are derived by summing up rows 1,…i, or by summing up rows i,…n in Eq. (8.70); in either case, most terms on the left-hand side cancel out because of the special structure of [K], as shown after Eq. (8.30).

While the oscillating terms of T_{gen} and T_{exc} are ignored in finding the initial angles of the mechanical part, they must be included in initializing the electromagnetic torques for solving the differential equations in the time-step loop. This is best done using

$$T_{gen\text{-}total}(0) = \lambda_d(0)\, i_q(0) - \lambda_q(0)\, i_d(0) \tag{8.73}$$

where the currents are

$$i_d(0) = i_{d\text{-}pos}(0) + i_{d\text{-}neg}(0)$$

$$i_q(0) = i_{q\text{-}pos}(0) + i_{q\text{-}neg}(0)$$

and the initial fluxes are calculated from Eq. (8.10). Similarly,

$$\omega T_{exc\text{-}total}(0) = -v_{f\text{-}pos}(0)\, i_f(0) + R_{exc}\,\{i_f(0)\}^2 \tag{8.74}$$

where

$$i_f(0) = i_{f-pos}(0) + i_{f-neg}(0)$$

8.5 Transient Solution

The numerical methods for the transient solution part are based on [13]. The basic idea is to reduce the machine equations to a three-phase Thevenin equivalent circuit, similar to that of Fig. 8.5 for the steady-state initialization. The equivalent circuit for the transient solution differs from Fig. 8.5 mainly in two aspects:

(a) The impedance matrix [Z] of Fig. 8.5 becomes a resistance matrix [R], after integrating the machine equations (8.9) with the trapezoidal rule of integration, and after reducing the seven equations for all windings to three equations for the armature windings.

(b) The sinusoidal voltage sources E" of Fig. 8.5 become instantaneous voltage sources which must be updated from step to step.

The updating procedure for the voltage sources requires the prediction of certain variables from the known solution at t - Δt to the yet unknown solution at t. Different prediction methods have been tried over the years, and their behavior with respect to numerical stability has gradually improved. Some earlier versions of the TYPE-59 synchronous machine model produced too much numerical noise [131], but beginning with version M36, the prediction methods are quite stable and the simulation results are fairly reliable now [132]. Further progress with respect to numerical stability can only be achieved if the overall EMTP algorithm is changed from a direct to an iterative solution in each time step.

8.5.1 Brief Outline of Solution Method

Assume that the solution at t - Δt is already known, and that the solution at t has to be found next. Then the method works roughly as follows:

(1) Predict the generator rotor angle β(t) (first predicted variable).

(2) Apply the trapezoidal rule of integration to the R-L branches of Fig. 8.2, in the direct axis as well as in the quadrature axis. Conceptually, this converts each R-L branch into an equivalent resistance in parallel with a known current source, as indicated in Fig. 8.10(a) and (b). The zero sequence consists of only one branch (Fig. 8.10(c)).

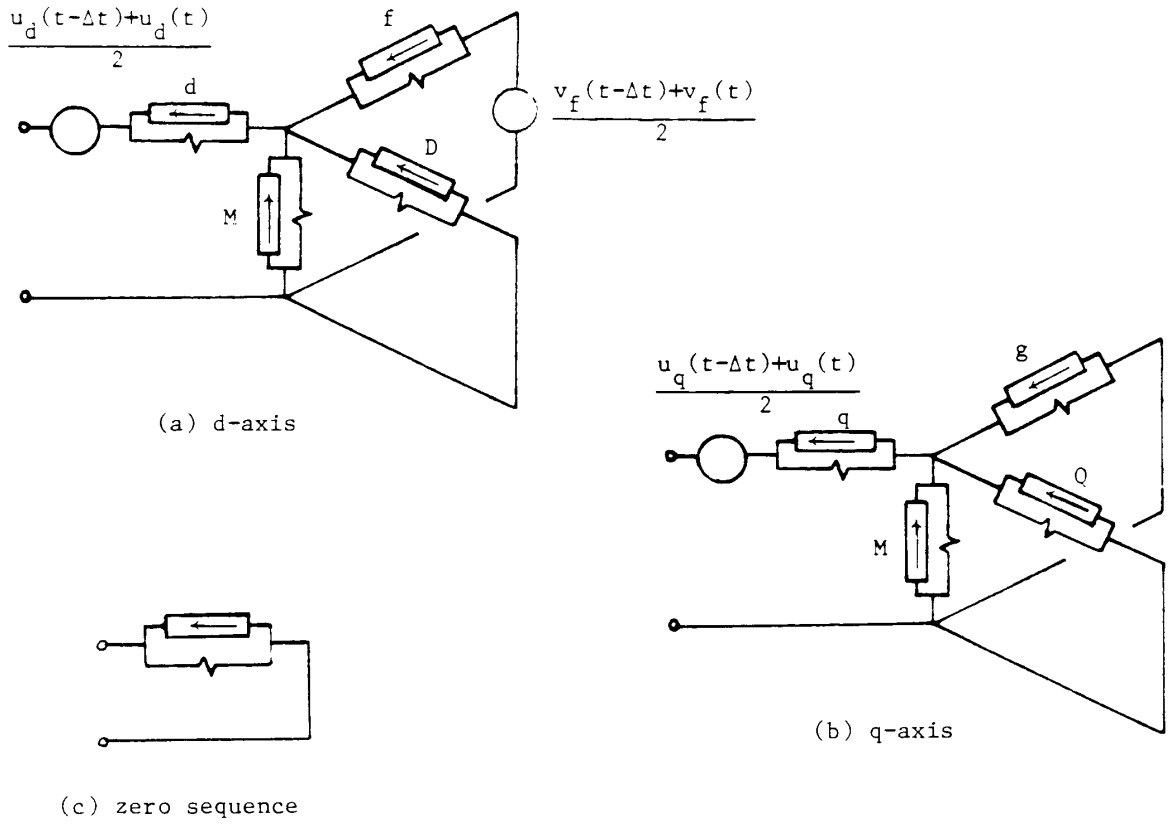

Fig. 8.10 - Resistive networks resulting from trapezoidal rule of integration (u = speed voltages defined in Eq. (8.75))

(3) Reduce the e- and q-axis resistive networks of Fig. 8.10 to one equivalent resistance in series with one equivalent voltage source as shown in Fig. 8.11. For this reduction, assume that $v_f(t) = v_f(t - \Delta t)$, which is exact if the excitation system is not modelled, or use some other prediction (e.g. linear extrapolation).

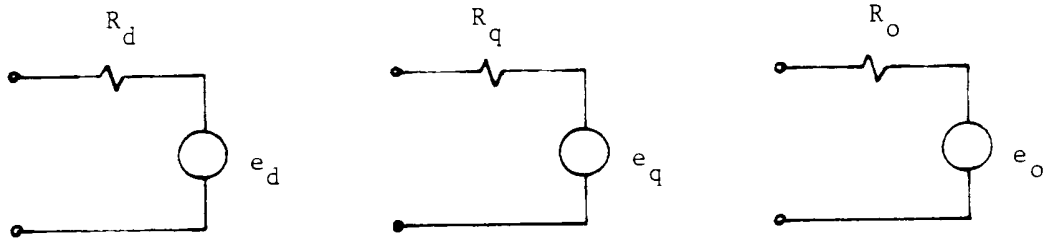

(a) Direct axis (b) Quadrature axis (c) Zero sequence

Fig. 8.11 - Resistive networks

Unfortunately, the speed voltages

$$u_d = -\omega \lambda_q$$

$$u_q = \omega \lambda_d \tag{8.75}$$

at time t are also unknown, but since fluxes can never change abruptly, their values can be predicted reasonably well. With predicted values for $u_d(t)$, $u_q(t)$ and $v_f(t)$ (2nd, 3rd and 4th predicted variable), the reduction is straightforward. Conceptually, branches M, f, D for the d-axis in Fig. 8.10(a) are paralleled, and then connected in series with the c-branch (analogous for the q-axis).

(4) Convert the 3 resistive Thevenin equivalent circuits for d, q, 0-quantities to phase quantities. If this were done directly, then the resulting 3 x 3 resistance matrix would be time-dependent as well as unsymmetric. To obtain a constant, symmetric matrix, the equivalent resistances of the d- and q-axis are averaged, as indicated in Fig. 8.12, and the "saliency terms" R_d-R_q / 2 • $i_d(t)$ and R_q-R_d / 2 • $i_q(t)$ are combined with the voltage sources e_d and e_q into one voltage source.

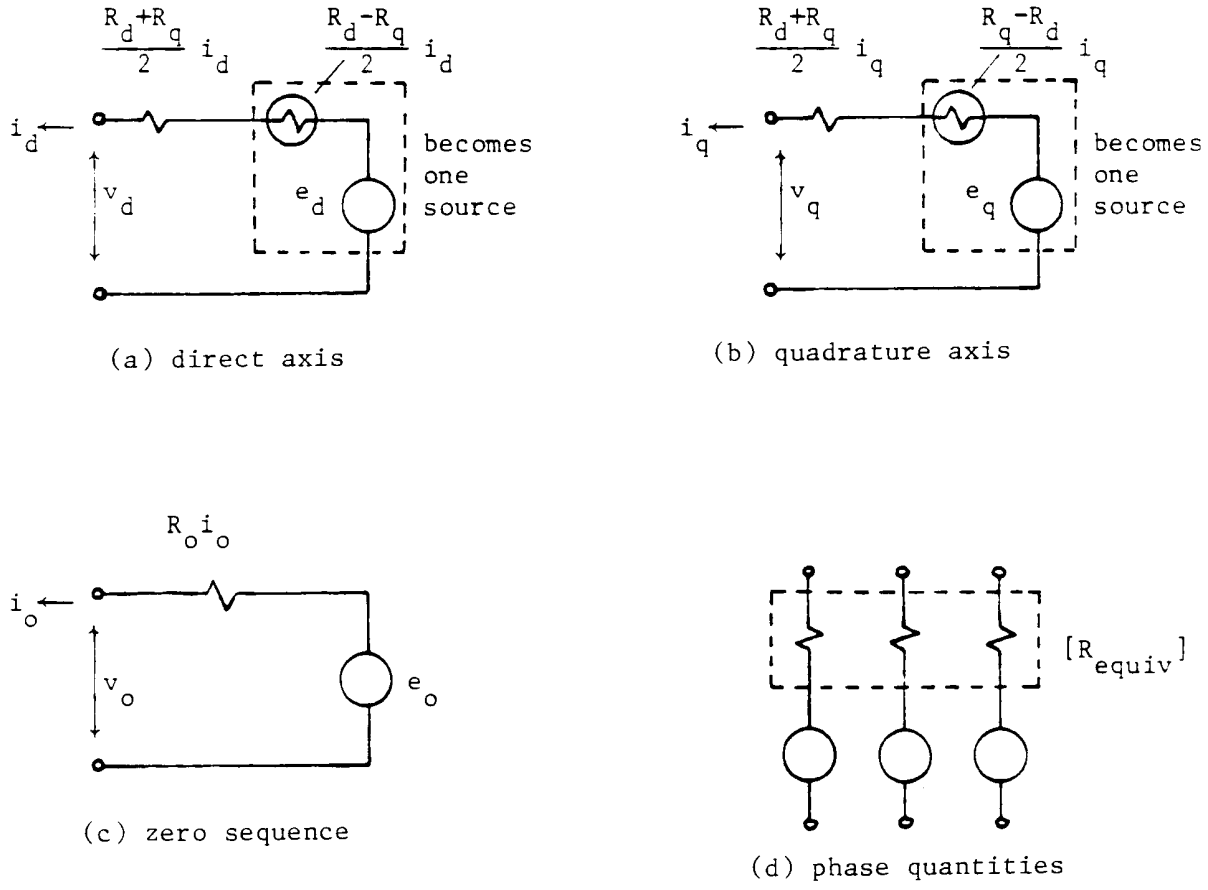

Fig. 8.12 - Modified resistive networks

This can only be done at the expense of having to use a predicted value for $i_d(t)$ and $i_q(t)$ (5th and 6th predicted variable). After conversion to phase quantities, the d, q, 0-networks become one three-phase network, with three source voltages behind a symmetric, constant resistance matrix

$[R_{equiv}]$.

(5) Solve the complete network, with the machine representation of Fig. 8.12(d). In the EMTP, current sources in parallel with $[R_{equiv}]$ are used in place of voltage sources in series with $[R_{equiv}]$.

(6) From the complete network solution in phase quantities, extract the generator voltages and convert them to d, q, 0-quantities. Calculate the armature currents in d, q, 0-quantities and the field structure currents, and use them to find the electromagnetic torques of the generator and exciter from Eq. (8.32) at time t. Then solve the equations of the mechanical part.

(7) Compare the predicted values of β, u_d, u_q, i_d, i_q with the corrected values from the solution of step (6), and repeat steps (6) and (7) if the difference is larger than the acceptable tolerance. When returning to step (6), it is assumed that the terminal voltages in phase quantities remain the same.

(8) Return to step (1) to find the solution at the next time step.

Some of the implementation details, which have been omitted from this brief outline, are discussed next. Variations of the iteration and prediction methods are described in Section 8.5.4.

8.5.2 Transient Solution of the Electrical Part

Consider the equations for the direct axis first, which are obtained from rows 1, 4, 6 of Eq. (8.9) and from Eq. (8.10a) as

$$\begin{bmatrix} v_d \\ v_f \\ 0 \end{bmatrix} = -\begin{bmatrix} R_a & & \\ & R_f & \\ & & R_d \end{bmatrix}\begin{bmatrix} i_d \\ i_f \\ i_D \end{bmatrix} - \begin{bmatrix} L_d & M_{df} & M_{dD} \\ M_{df} & L_{ff} & M_{fD} \\ M_{dD} & M_{fD} & L_{DD} \end{bmatrix}\begin{bmatrix} di_d/dt \\ di_f/dt \\ di_D/dt \end{bmatrix} + \begin{bmatrix} u_d \\ 0 \\ 0 \end{bmatrix} \tag{8.76a}$$

with u_d being the speed voltage from Eq. (8.75), or in short-hand notation,

$$[v] = -[R]\,[i] - [L]\left[\frac{di}{dt}\right] + [u] \tag{8.76b}$$

Because of numerical noise problems in pre-M32 versions of the BPA EMTP, this equation is integrated with the "damped trapezoidal rule" of Section 2.2.2[11], with a damping resistance matrix $[R_p]$ in parallel with [L],

$$[R_p] = \frac{1 + \alpha}{1 - \alpha} \cdot \frac{2}{\Delta t}\,[L] \tag{8.77}$$

where α is the reciprocal of the damping factor defined in Eq. (2.21). For $\alpha = 1$ there is no damping, while $\alpha = 0$ is the critically damped case. In the present version of the BPA EMTP, a default value of $(1 + \alpha)/(1 - \alpha) = 100$ is used.

---

[11]The (unreleased) UBC version with synchronous machines uses the normal trapezoidal rule. By setting $\alpha = 1$ in the input, the BPA EMTP would use the normal trapezoidal rule as well.

Applying the damped trapezoidal rule of Eq. (2.20) for v = L di/dt to Eq. (8.76), with v replaced by [u] - [v] - [R][i], results in

$$[v(t)] = [u(t)] + [hist(t-\Delta t)] - \{[R] + \frac{1+\alpha}{\Delta t}[L]\}[i(t)] \tag{8.78a}$$

with the known history term

$$[hist(t-\Delta t)] = \{-\alpha[R] + \frac{1+\alpha}{\Delta t}[L]\}[i(t-\Delta t)] - \alpha[v(t-\Delta t)] + \alpha[u(t-\Delta t)] \tag{8.78b}$$

Eq. (8.78a) described a voltage source [u(t)] + [hist(t - Δt)] behind a resistance matrix

$$[R_{comp}] = [R] + \frac{1+\alpha}{\Delta t}[L] \tag{8.79}$$

Subscript "comp" is used because such equivalent resistive networks are called "resistive companion models" in network theory [133].

For interfacing the synchronous machine equations with the network equations, the field structure quantities are eliminated from Eq. (8.78). Dropping subscript "comp" and using subscripts d, f, D again, the field structure currents can be expressed from the last two rows of Eq. (8.78a) with $[R_{comp}]$ from Eq. (8.79) as

$$\begin{bmatrix} i_f(t) \\ i_D(t) \end{bmatrix} = \begin{bmatrix} R_{ff} & R_{fD} \\ R_{fD} & R_{DD} \end{bmatrix}^{-1} \left[\begin{bmatrix} hist_f(t-\Delta t) \\ hist_D(t-\Delta t) \end{bmatrix} - \begin{bmatrix} v_f(t) \\ 0 \end{bmatrix} - \begin{bmatrix} R_{df} \\ R_{dD} \end{bmatrix} i_d(t) \right] \tag{8.80}$$

which, when inserted into the first row of Eq. (8.78a), produces a single equation for the d-axis,

$$v_d(t) = e_d - R_d\, i_d(t) \tag{8.81}$$

with the reduced companion resistance

$$R_d = R_{dd} - [R_{df} \quad R_{dD}] \begin{bmatrix} R_{ff} & R_{fD} \\ R_{fD} & R_{DD} \end{bmatrix}^{-1} \begin{bmatrix} R_{df} \\ R_{dD} \end{bmatrix} \tag{8.82a}$$

the voltage source

$$e_d = u_d(t) + hist_d^{red}(t - \Delta t) \tag{8.82b}$$

and the reduced history term

$$hist_d^{red} = hist_d - [R_{df} \quad R_{dD}] \begin{bmatrix} R_{ff} & R_{fD} \\ R_{fD} & R_{DD} \end{bmatrix}^{-1} \begin{bmatrix} hist_f - v_f(t) \\ hist_D \end{bmatrix} \tag{8.82c}$$

By predicting the speed voltage $u_d(t) = -\omega(t)\lambda_q(t)$, and by assuming that $v_f(t) = v_f(t - \Delta t)$, the simple resistive network of Fig. 8.11(a) is obtained, with a voltage source e_d behind the companion resistance R_d. If $R << 2L/\Delta t$ in all R-L branches of Fig. 8.10(a), then

$$R_d \approx \frac{2L_d''}{\Delta t} \tag{8.83a}$$

Therefore, Eq. (8.81) essentially represents the trapezoidal rule solution of a voltage source behind the subtransient reactance X_d''. In publications based on [13]. R_d is called a_{11}.

If the dynamic behavior of the excitation system is to be simulated as well, then using $v_f(t) = v_f(t - \Delta t)$ implies a one time-step delay in the effect of the excitation system on the machine. Such a delay is usually acceptable, because Δt is typically much smaller than the effective time constant between the input and output of the excitation systems. Alternatively, some type of prediction could be used for $v_f(t)$.

The derivations for the q-axis are obviously analogous to those just described for the d-axis, and lead to the single equation for the q-axis,

$$v_q(t) = e_q - R_q i_q(t) \tag{8.84}$$

with the voltage source

$$e_q = u_q(t) + hist_q^{red}(t - \Delta t) \tag{8.85}$$

Here, only the speed voltage $u_q(t) = \omega(t)\lambda_d(t)$ must be predicted because the voltage $v_g(t)$ is zero. The q-axis resistive network is shown in Fig. 8.11(b). Again, if $R << 2L/\Delta t$ in all R-L branches of Fig. 8.10(b), then

$$R_q \approx \frac{2L_q''}{\Delta t} \tag{8.83b}$$

Therefore, Eq. (8.84) essentially represents the trapezoidal rule solution of a voltage source behind the subtransient reactance X_q''. In publications based on [13], R_q is called a_{22}.

The equations for the zero sequence quantities (row 3 in Eq. (8.9) and Eq. (8.10c)) are also integrated with the damped trapezoidal rule, which leads to

$$v_0(t) = hist_0(t - \Delta t) - R_0 i_0(t) \tag{8.86a}$$

with the companion resistance

$$R_0 = R_a + \frac{1 + \alpha}{\Delta t} L_0 \tag{8.86b}$$

and the known history term

$$hist_0(t-\Delta t) = \left(\frac{1+\alpha}{\Delta t} L_0 - \alpha R_a \right) i_0(t-\Delta t) - \alpha v_0(t-\Delta t) \tag{8.86c}$$

The zero sequence resistive network of Eq. (8.86a) with $e_0 = hist_0(t - \Delta t)$ is shown in Fig. 8.11(c). In publications based on [13]. R_0 is called a_{33}.

The reduced generator equations (8.81), (8.84) and (8.86a) can be solved in one of two ways:

(1) Find a three-phase Thevenin equivalent circuit (resistive companion model) for the network seen from the generator terminals, and solve it together with the generator equations.

(2) Add the reduced generator equations to the network equations, and solve them simultaneously.

The first approach was used in [98]. It has the advantage that iterations can easily be implemented for the correction of predicted values. However, generator must be separated by distributed-parameter lines with travel time for reasons of numerical efficiency, so that an independent three-phase Thevenin equivalent circuit can be generated for each generator (otherwise, M generators would have to be interfaced with one 3 x M-phase Thevenin equivalent circuit). If there are no such lines in reality, artificial stub-lines with $\tau = \Delta t$ must be used to separate the generators. This can result in incorrect answers. For this reason, the first approach has been abandoned in the EMTP.

With the second approach, there is no restriction on the number of generators connected to the network, or even to the same bus. However, it does require the prediction of certain variables, which makes this approach more sensitive to the accumulation of prediction errors. It is the only method retained in the present BPA EMTP, and only this method is discussed here. To solve the generator equations with the network equations, the generator resistive networks of Fig. 8.12 in d, q, 0-quantities must be converted to phase quantities, which produces a time-dependent and unsymmetric 3 x 3 resistance matrix. To accommodate such matrices would have required a complete restructuring of the basic (non-iterative) solution algorithm of the EMTP. Instead, an average resistance

$$R_{av} = (R_d + R_q)/2 \tag{8.87}$$

is used on both axes. This requires "saliency terms" $i_d(R_d\text{-}R_q)/2$ on the d-axis and $i_q(R_q\text{-}R_d)/2$ on the q-axis, which are added to the known voltage sources e_d, e_q by using predicted values for i_d, i_q (Fig. 8.12). For generators with $X_d" = X_q"$, these saliency terms are practically negligible. For the IEEE benchmark model [74] with different values of $X_d" = 0.135$ p.u. and $X_q" = 0.200$ p.u., the companion resistances are $R_d = 3.5844$ p.u. and $R_q = 5.3103$ p.u. for $\Delta t = 200\ \mu s$. These values are practically identical with $2L_d"/\Delta t = 3.5810$ p.u. and $2L_q"/\Delta t = 5.3052$ p.u., as mentioned in Eq. (8.83). The voltage drop across the saliency terms $(R_d\text{-}R_q)/2$ would be 20% of the voltage drop across $(R_d+R_q)/2$ with $\Delta t = 200\ \mu s$.

With the average resistance of Eq. (8.87), the modified equations in d, q, 0-quantities become

$$\begin{bmatrix} v_d(t) \\ v_q(t) \\ v_0(t) \end{bmatrix} = \begin{bmatrix} e_{d\text{-mod}} \\ e_{q\text{-mod}} \\ e_0 \end{bmatrix} - \begin{bmatrix} R_{av} & & \\ & R_{av} & \\ & & R_0 \end{bmatrix} \begin{bmatrix} i_d(t) \\ i_q(t) \\ i_0(t) \end{bmatrix} \tag{8.88a}$$

where

$$e_{d-\mathrm{mod}} = e_d - \frac{R_d - R_q}{2} i_d(t) \tag{8.88b}$$

$$e_{q-\mathrm{mod}} = e_q + \frac{R_d - R_q}{2} i_q(t) \tag{8.88c}$$

Predicted values i_d, i_q are used in the last two equations, and the voltage sources behind resistances are then converted into current sources in parallel with the resistances,

$$i_{d-source} = \frac{1}{R_{av}} e_{d-\mathrm{mod}} \tag{8.89a}$$

$$i_{q-source} = \frac{1}{R_{av}} e_{q-\mathrm{mod}} \tag{8.89b}$$

$$e_{0-source} = \frac{1}{R_0} e_0 \tag{8.89c}$$

Finally, the d, q, 0-quantities are converted to phase quantities with a predicted angle $\beta(t)$, which produces a resistive companion model with current sources

$$\begin{bmatrix} i_{1-source} \\ i_{2-source} \\ i_{3-source} \end{bmatrix} = \frac{\sqrt{2}}{\sqrt{3}} \begin{bmatrix} \cos\beta & \sin\beta & \frac{1}{\sqrt{2}} \\ \cos(\beta-120^\circ) & \sin(\beta-120^\circ) & \frac{1}{\sqrt{2}} \\ \cos(\beta+120^\circ) & \sin(\beta+120^\circ) & \frac{1}{\sqrt{2}} \end{bmatrix} \begin{bmatrix} i_{d-source} \\ i_{q-source} \\ i_{0-source} \end{bmatrix} \tag{8.90}$$

and parallel with

$$[R_{equiv}] = \begin{bmatrix} R_s & R_m & R_m \\ R_m & R_s & R_m \\ R_m & R_m & R_s \end{bmatrix} \tag{8.91a}$$

where

$$R_s = (R_0 + 2R_{av})/3\,, \qquad R_m = (R_0 - R_{av})/3 \tag{8.91b}$$

Since this model is identical with the resistive companion model of Eq. (3.8) for coupled inductances, generators are interfaced with the network equations as if they were coupled inductances. The matrix $[R_{equiv}]^{-1}$ enters the nodal conductance matrix [G] of Eq. (1.8) once and for all outside the time step loop, while the parallel current sources are updated from step to step.

After the complete network solution has been obtained at time t, the generator phase voltages are converted

to d, q, 0-quantities,

$$\begin{bmatrix} v_d \\ v_q \\ v_0 \end{bmatrix} = \frac{\sqrt{2}}{\sqrt{3}} \begin{bmatrix} \cos\beta & \cos(\beta-120°) & \cos(\beta+120°) \\ \sin\beta & \sin(\beta-120°) & \sin(\beta+120°) \\ 1\sqrt{2} & 1\sqrt{2} & 1\sqrt{2} \end{bmatrix} \begin{bmatrix} v_1 \\ v_2 \\ v_3 \end{bmatrix} \tag{8.92}$$

and the armature currents are found from

$$\begin{aligned} i_d &= (e_{d\text{-mod}} - v_d)/R_{av} \\ i_q &= (e_{q\text{-mod}} - v_q)/R_{av} \\ i_0 &= (e_0 - v_0)/R_0 \end{aligned} \tag{8.93}$$

The field structure currents are recovered from Eq. (8.80) for the d-axis, and from an analogous equation for the q-axis. Finally, the fluxes λ_d, λ_q are calculated from Eq. (8.10a) and (8.10b), and the electromagnetic torques from Eq. (8.32), which are then used to solve the mechanical equations as described next.

8.5.3 Transient Solution of the Mechanical Part

The mechanical part is described by Eq. (8.29), which can be rewritten as

$$[J]\left[\frac{d\omega}{dt}\right] + [D][\omega] + [K][\theta] = [T_{net}] \tag{8.94a}$$

with the speeds of the system of masses

$$[\omega] = \left[\frac{d\theta}{dt}\right] \tag{8.94b}$$

and the net torque

$$[T_{net}] = [T_{turbine}] - [T_{gen/exc}] \tag{8.94c}$$

The torque $[T_{gen/exc}]$ provides the only direct link with the electrical part, with another indirect link through $\theta_{gen} = \beta$ which had to be predicted to solve the electrical part.

Applying the trapezoidal rule (or central difference quotients) to Eq. (8.94a) and (8.94b) yields

$$[J]\frac{[\omega(t)] - [\omega(t-\Delta t)]}{\Delta t} + [D]\frac{[\omega(t)] + [\omega(t-\Delta t)]}{2} + [K]\frac{[\theta(t)] + [\theta(t-\Delta t)]}{2}$$

$$= \frac{[T_{net}(t)] + [T_{net}(t-\Delta t)]}{2} \tag{8.95}$$

and

$$\frac{[\omega(t)] + [\omega(t-\Delta t)]}{2} = \frac{[\theta(t)] - [\theta(t-\Delta t)]}{\Delta t} \tag{8.96}$$

Replacing [θ(t)] in Eq. (8.95) with the expression from Eq. (8.96) produces

$$\left\{\frac{2}{\Delta t}[J] + [D] + \frac{\Delta t}{2}[K]\right\}[\omega(t)] = [T_{net}(t)] + [hist(t-\Delta t)] \tag{8.97a}$$

with the known history term

$$[hist(t-\Delta t)] = \left\{\frac{2}{\Delta t}[J] - [D] - \frac{\Delta t}{2}[K]\right\}[\omega(t-\Delta t)] - 2[K][\theta(t-\Delta t)] + [T_{net}(t-\Delta t)] \tag{8.97b}$$

Normally, it is assumed that the turbine power is constant. In that case, the torque on each mass i is calculated by using predicted speeds ω_i,

$$T_{turbine,\,i} = \frac{P_{turbine,\,i}}{\omega_i} \tag{8.98}$$

If constant turbine torque is assumed, then Eq. (8.98) is skipped. With the turbine torques from Eq. (8.98), and with the electromagnetic torques at time t already calculated in the electrical part, Eq. (8.97a) can be solved directly for the speeds [ω(t)]. The matrices

$$[A] = \frac{2}{\Delta t}[J] + [D] + \frac{\Delta t}{2}[K] \qquad \textit{and} \qquad [B] = \frac{2}{\Delta t}[J] - [D] - \frac{\Delta t}{2}[K]$$

are tridiagonal, and remain constant from step to step. They are triangularized once and for all before entering the time step loop, with a Gauss elimination subroutine specifically written for tridiagonal matrices, which saves storage as well as computer time. Inside the time step loop, the information in the triangularized matrix is used to apply the elimination to the right-hand sides, followed by backsubstitution ("repeat solution," as explained in Section III.1).

It is worth noting that the form of Eq. (8.94) is the same as the system of branch equations for coupled R-L-C branches. In that analogy, the matrix [J] is equivalent to a matrix [L] of uncoupled inductances, the matrix [D]

to a matrix [R] of coupled resistances, and the matrix [K] to an inverse capacitance matrix $[C]^{-1}$ of coupled capacitances. $[T_{net}]$ would be equivalent to the derivatives [dv/dt] of the applied branch voltages.

8.5.4 Prediction and Correction Schemes

The synchronous machine code in the EMTP has undergone many changes, especially with respect to the prediction and correction schemes. The presently used schemes, as well as variations of it, are summarized here.

8.5.4.1 Prediction of ω and β

The speeds of all masses are predicted with linear extrapolation,

$$[\omega(t)] = 2\,[\omega(t - \Delta t)] - [\omega(t - 2\Delta t)] \tag{8.99}$$

Since the speeds change slowly, in comparison with the electrical quantities, this prediction should be accurate enough. Predicted speeds are needed in two places, namely for the prediction of speed voltages (see Section 8.5.4.3), and for the calculation of turbine torques from Eq. (8.98). The accuracy of the predicted generator rotor speed ω_{gen} is more important because there is no speed voltage correction in the present iteration scheme. The accuracy of the turbine rotor speeds prediction is less important, because the torque calculations Eq. (8.98) are corrected in the iteration scheme of Section 8.5.1, if constant turbine power is assumed (default option in UBC EMTP, only option in BPA EMTP). If constant turbine torque is assumed, then the turbine speed predictions are not needed at all.

Fig. 8.13 shows the speed and the electromagnetic torque of a generator by itself (no turbine connected to it), which runs unloaded at synchronous speed and is then switched into a resistance load at t = 0 [134] (data in Table 8.2). The generator slows down very quickly in this case. The curves were obtained with the UBC EMTP without iterations (no return from step 7 to 6 in Section 8.5.1), and verified with a 4th-order Runge-Kutta-Merson method (agreement to within 4 digits). Both the UBC and BPA EMTP had bugs in the speed calculation, which were not noticed before in cases of small speed changes. They were corrected after J. Mechenbier proved their existence by using principles of energy conservation as suggested by H. Boenig and S. Ranade [134].

The angle β of the generator rotor must be predicted so that the d, q, 0-networks of Fig. 8.12 can be converted to phase quantities for the complete network solution in step 5 of Section 8.5.1. There is no correction for this conversion in the present iteration scheme. The angle β is also needed for converting the voltage solution back from phase to d, q, 0-quantities in step 6 of Section 8.5.1; here, corrected values are obtained from the solution of the mechanical part if steps (6) and (7) are iterated.

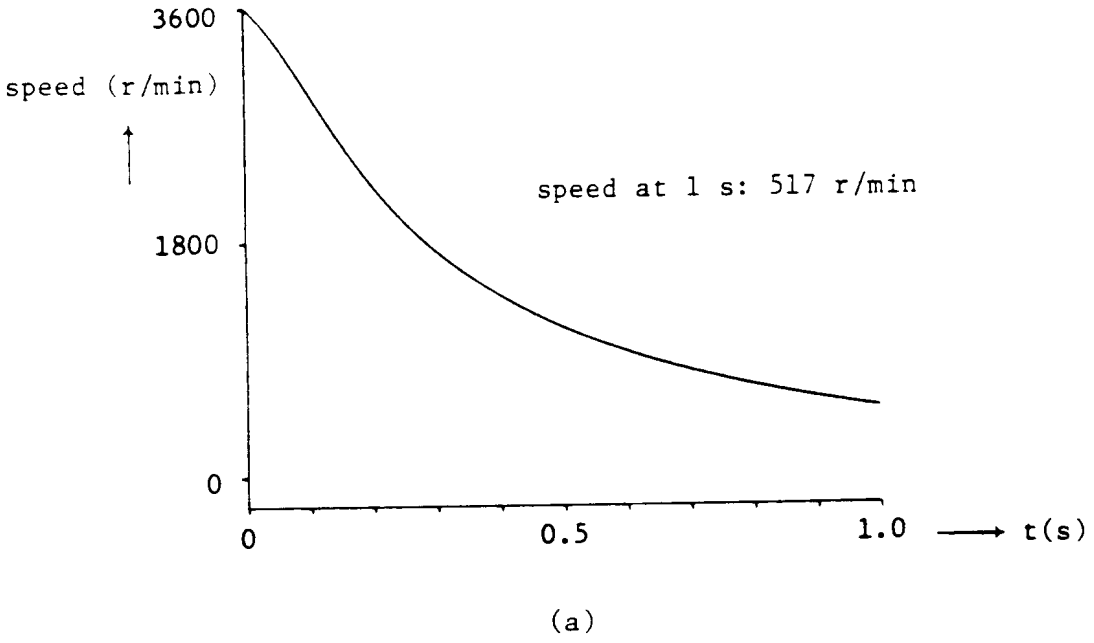

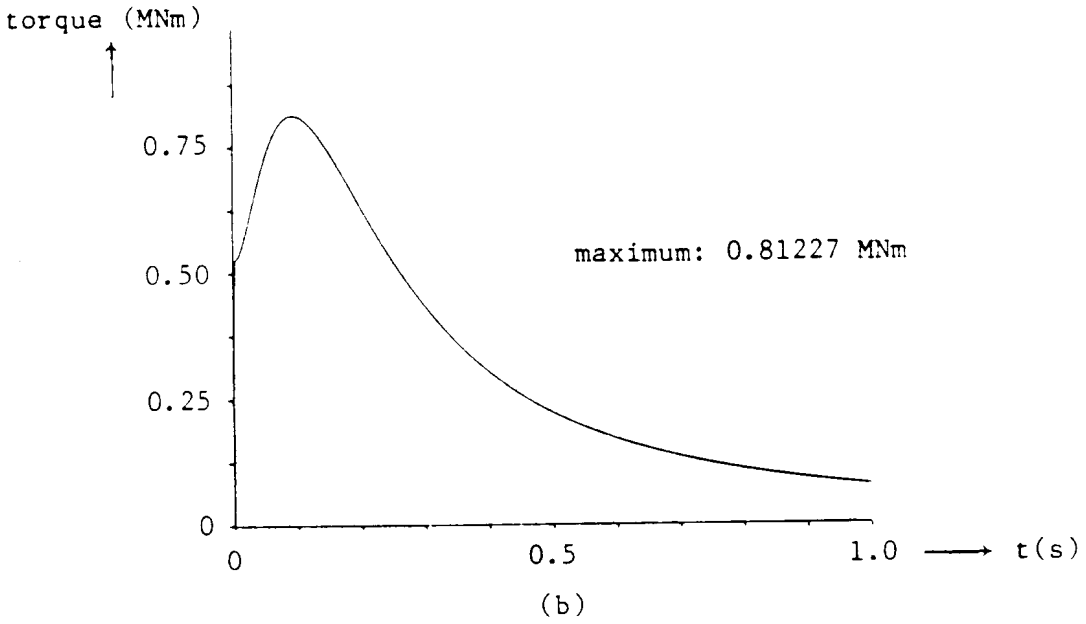

Fig. 8.13 - Speed and electromagnetic torque of an unloaded generator when switched into a resistance load. (a) Speed, (b) Electromagnetic torque.

In the UBC EMTP, the predicted value for β is calculated from the predicted speed ω_{gen} with the trapezoidal rule of integration (8.96),

$$\beta(t) = \beta(t - \Delta t) + \frac{\Delta t}{2}\{\omega_{gen}(t - \Delta t) + \omega_{gen}(t)\} \tag{8.100}$$

M36 and later versions of the BPA EMTP use a predictor formula suggested by Kulicke [135], which is based on the assumption that β is a fourth-order polynomial of t,

$$\beta = a_0 + a_1 t + a_2 t^2 + a_3 t^3 + a_4 t^4 \tag{8.101}$$

By using three known values of β at t - Δt, t - 2Δt, t - 3Δt, and two known values of the speed

$$\omega = \frac{d\beta}{dt} = a_1 + 2a_2 t + 3a_3 t^2 + 4a_4 t^3 \tag{8.102}$$

at t - Δt, t - 2Δt, the coefficients $a_0,\ldots a_4$ can be found from the solution of 5 linear equations. This is a Hermite interpolation formula and leads to the predictor formula [7; p. 184, P6 in Table 5.1]

$$\beta(t) = -9\{\beta(t-\Delta t) - \beta(t-2\Delta t)\} + \beta(t-3\Delta t) + 6\Delta t\{\omega_{gen}(t-\Delta t) + \omega_{gen}(t-2\Delta t)\} \tag{8.103}$$

Table 8.2 - Generator test case no. 1 [134]

Ratings:	160 MVA (three-phase), 15 kV (line-to-line), wye-connected.
Reactances:	$X_d = 1.7$ p.u., $X_d' = 0.245$ p.u., $X_d'' = 0.185$ p.u.
	$X_q = 1.64$ p.u., $X_q'' = 0.185$ p.u. (no g-winding)
	$X_\ell = 0.15$ p.u., $X_O = 0.14$ p.u.
Time constants:	$T_{do}' = 5.9$ s, $T_{do}'' = 0.03046$ s
	$T_{qp}'' = 0.075$ s
Resistances:	$R_a = 0.001096$ p.u.
	$R_{load} = 10^8\ \Omega$ in steady state (no effect; added because some versions cannot handle isolated generator)
	$R_{load} = 1\ \Omega$ after switching at t = 0
Moment of inertia:	$J = 999.947$ (N-m)s^2. One pole pair.
Terminal voltage:	$V_1 = 12.247\, e^{j216^\circ}$ kV (peak) in steady state in phase 1 (symmetrical in 3 phases).
Step size	$\Delta t = 200\ \mu$s. f = 60 Hz

With coefficients $a_0,\ldots a_4$ known, a predictor formula for $\omega_{gen} = d\beta/dt$ for use in the speed voltages could be written down with Eq. (8.102) as well,

$$\Delta t\,\omega(t) = 14\Delta t\,\omega(t-\Delta t) + 17\Delta t\,\omega(t-2\Delta t) - 27\beta(t-\Delta t) + 24\beta(t-2\Delta t)$$

$$+ 3\beta(t-3\Delta t) \tag{8.104}$$

The BPA EMTP uses the predicted speed from Eq. (8.99), though. It is not clear whether the 4th order predictor of Eq. (8.103) is really superior to the predictor of Eq. (8.99).

8.5.4.2. Averaging of d- and q-Axis Companion Resistances

Instead of an average resistance ($R_d + R_{q\_}/2$ in Fig. 8.12, the M39 version of the BPA EMTP uses R_d on both d- and q-axes. To compensate for this, a term $(R_q\text{-}R_d) \bullet i_q$ is added to the voltage source on the q-axis, and no compensating term is needed on the d-axes. Whether this method is better than the averaging procedure of Fig. 8.12 is unclear. Both procedures are special cases of a class of averaging methods discussed in [136].

8.5.4.3. Prediction of i_d, i_q

The armature currents i_d, i_q must be predicted so that the saliency terms $i_d(R_d\text{-}R_q)/2$ and $i_q(R_q\text{-}R_d)/2$ can be combined with the known voltage sources e_d, e_q (Fig. 8.12). No correction is made for this in the present iteration scheme. Note that the saliency terms are practically zero if $X_q" = X_d"$. In the UBC version and in BPA versions until M32, the predicted currents i_d, i_q are also used to find predicted speed voltages, as described in the next section. In the UBC EMTP, linear extrapolation is used,

$$i(t) = 2i(t - \Delta t) - i(t - 2\Delta t) \tag{8.105}$$

where "i" is either i_d or i_q. The BPA version uses a linear three-point predictor formula which smoothes numerical oscillations. With the current known at t - Δt, t - 2Δt and t - 3Δt as

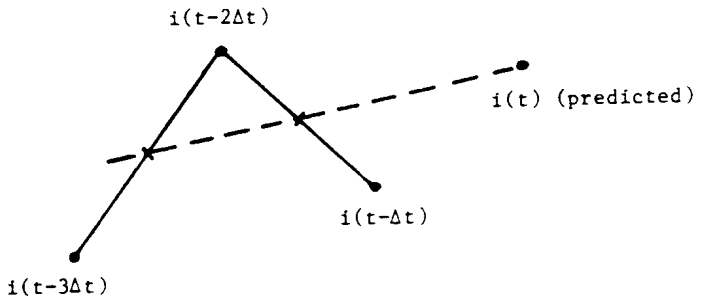

Fig. 8.14 - Linear prediction with smoothing

indicated in Fig. 8.14, averaged values are first found at the two midpoints by linear interpolation

$$i(t - 2\frac{1}{2}\Delta t) = \frac{i(t - 3\Delta t) + i(t - 2\Delta t)}{2}$$

$$i(t - 1\frac{1}{2}\Delta t) = \frac{i(t - 2\Delta t) + i(t - \Delta t)}{2}$$

Then a straight line is drawn through the two midpoints, with a slope of

$$slope = \frac{i(t - \Delta t) - i(t - 3\Delta t)}{2\,\Delta t}$$

to predict the current i(t),

$$i(t) = \frac{5}{4} i(t - \Delta t) + \frac{1}{2} i(t - 2\Delta t) - \frac{3}{4} i(t - 3\Delta t) \tag{8.106}$$

This linear prediction with smoothing is conceptually similar to fitting a straight line through three points in the least squares sense. Such a straight line least square fitting would have the same slope, but a value at t - 2Δt of {i(t - 3Δt) + i(t - 2Δt) + i(t - Δt)}/3 instead of {i(t - 3Δt) + 2i(t - 2Δt) + i(t - Δt)}/4 in Fig. 8.14, which would yield a predictor

$$i(t) = \frac{4}{3} i(t - \Delta t) + \frac{1}{3} i(t - 2\Delta t) - \frac{2}{3} i(t - 3\Delta t) \tag{8.107}$$

Which predictor performs best is difficult to say. All predictor formulas discussed in this section depend solely on past points, and not on the form of the differential equations for i_d, i_q. Eq. (8.76), and an analog equation for the q-axis, were tried at one time as Euler predictor formulas, but they performed worse than the predictors discussed here. It might be worth exploring other predictor formulas, because the accuracy of the solution depends primarily on the prediction of i_d, i_q, especially if the speed voltages are calculated from i_d, i_q as well, as discussed in the next section. One could use Eq. (8.103), for example, by replacing β with i and ω with di/dt calculated from Eq. (8.76).

Fig. 8.15 shows the current in phase 1 after a three-phase short-circuit of a generator with unrealistically low armature resistance $R_a = 0.0001$ p.u. The data for this case is summarized in Table 8.3. Since speed changes were ignored, the only predicted values are i_d, i_q, as well as speed voltages in the BPA EMTP.

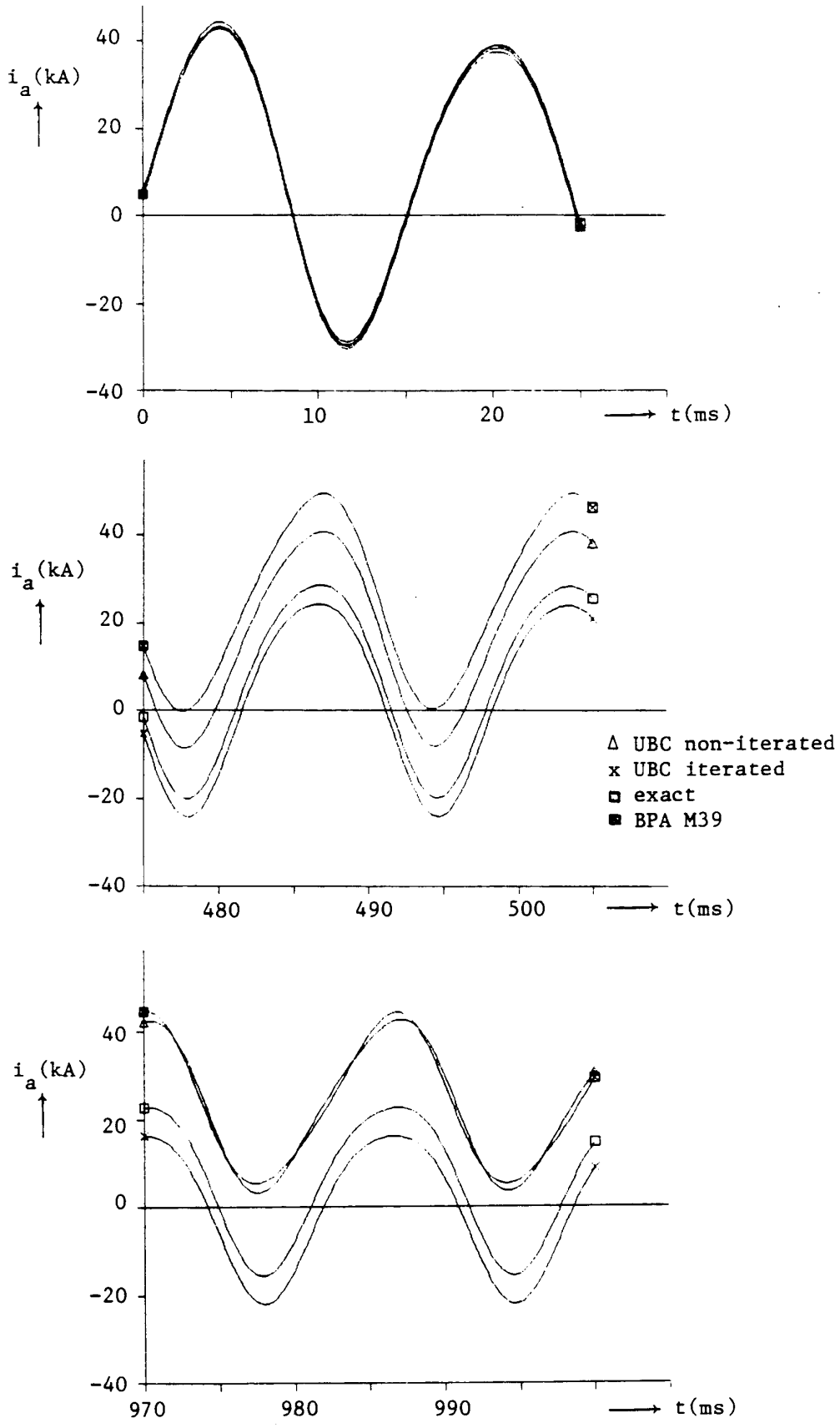

Fig. 8.15 - Current in phase 1 after a three-phase short-circuit. R_a = 0.0001 p.u.

Table 8.3 - Generator test case no. 2

Ratings:	400 MVA (three-phase), 18 kV (line-to-line), wye-connected
Reactances:	$X_d = 0.92$ p.u., $X_d' = 0.18$ p.u., $X_d'' = 0.161$ p.u.
	$X_q = 0.748$ p.u., $X_q'' = 0.161$ p.u. (no g-winding)
	$X_l = X_O = 0.082$ p.u.
Time constants:	$T_{do}' = 6.6$ s, $T_{do}'' = 0.05$ s
	$T_{qO}'' = 0.05$ s
Resistances:	$R_a = 10^{-4}$ p.u. (unrealistically low value)
	$R_a = 10^{-3}$ p.u. (more realistic value)
	$R_{load} = 1\ \Omega$
Moment of inertia:	$J = \infty$ (constant speed)
Terminal voltage:	$V_1 = 4.926\ e^{j\,7.391^\circ}$ kV (peak) in steady state in phase 1 (symmetrical in 3 phases).
Step size	$\Delta t = 200\ \mu$s. f = 60 Hz
Disturbance:	Three-phase short-circuit at terminals at t = 0

In such a case with low damping, the errors caused by the prediction do accumulate noticeably if the simulation runs over 5000 steps to $t_{max} = 1$ s. The errors are decreased if the complete network solution is iterated (not yet available as an option in the production codes of the EMTP). For comparison purposes, the exact solution is shown as well, which was found for i_d, i_q, with the eigenvalue/eigenvector method discussed in Appendix I.1, and then transformed to phase quantities with β from Eq. (8.23). Fig. 8.16 shows the results if the armature resistance is changed to a more realistic value of $R_a = 0.001$ p.u. As can be seen, the answers are now closer to the exact solution.

8.5.4.4. Prediction of Speed Voltages

Starting with M32 of the BPA EMTP, the speed voltages u_d, u_q of Eq. (8.75) are predicted in the same way as i_d, i_q with Eq. (8.106). In some of these versions, the prediction was done in a synchronously rotating reference frame, and then converted directly to phase quantities without going through d, q-axes parameters. This has been abandoned in Feb. 1986, and the speed voltages are now again predicted in d, q-quantities because the latter turned out to be superior when applied to test case no. 1 of Table 8.2.

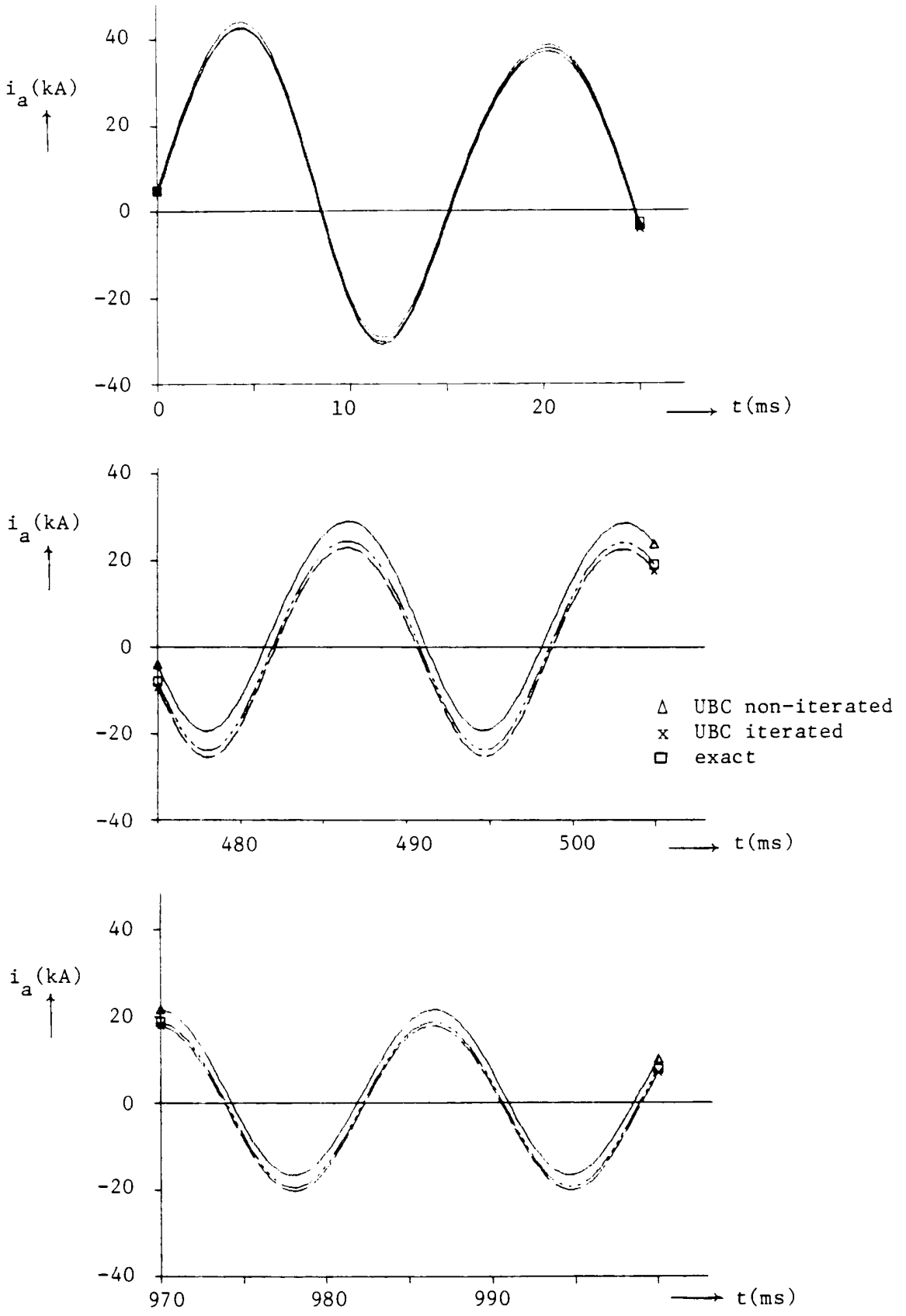

Fig. 8.16 - Current in phase 1 after a three-phase short-circuit. R_a = 0.001 p.u.

In pre-M32 versions of the BPA EMTP, and in the (unreleased) UBC version with synchronous machines, the speed voltages $u_d = -\omega\lambda_q$ and $u_q = \omega\lambda_d$ are not predicted explicitly. Instead, the predicted currents $i_d(t)$, $i_q(t)$ and the predicted speed $\omega_{gen}(t)$ are used to calculate the speed voltages from Eq. (8.10a) and (8.10b). The field structure currents appearing in these equations are expressed as a function of i_d with Eq. (8.80), which leads to the expression

$$\lambda_d(t) = L_d^{reduced}\, i_d(t) + \lambda_{d\text{-}0} \tag{8.108}$$

with the known reduced inductance

$$L_d^{reduced} = L_d - [L_{df} \quad L_{dD}] \begin{bmatrix} R_{ff} & R_{fD} \\ R_{fD} & R_{DD} \end{bmatrix}^{-1} \begin{bmatrix} R_{df} \\ R_{dD} \end{bmatrix} \tag{8.109}$$

and the known flux $\lambda_{d\text{-}0}$ for zero current ($i_d = 0$),

$$\lambda_{d\text{-}0} = [L_{df} \quad L_{dD}] \begin{bmatrix} R_{ff} & R_{fD} \\ R_{fD} & R_{DD} \end{bmatrix}^{-1} \begin{bmatrix} hist_f - v_f(t) \\ hist_D \end{bmatrix} \tag{8.110}$$

The reduced inductance $L_d^{reduced}$ is practically identical with L_d'' if $R << 2L/\Delta t$. For the IEEE benchmark model [74] with $\Delta t = 200\ \mu s$, $\omega L_d = 0.135129$ p.u. compared to $\omega L_d'' = 0.135$ p.u. In publications based on [13], $\omega L_d^{reduced}$ is called $-a_{21}$ and $\omega L_q^{reduced}$ is called a_{12}.

8.5.4.5. Iteration Schemes

Up to now, the complete network solution is direct, without iterations. The iteration scheme of Section 8.5.1 does not repeat the network solution, and predicted values are therefore never completely corrected. There is only one exception, namely the three-phase short-circuit at the generator terminals with zero fault resistance. In that case the terminal voltages are always zero, and going back to step 6 in the iteration scheme of Section 8.5.1 should be a complete correction of all predicted values.

It is doubtful whether the predictors can be improved much more. Further improvements can probably only be made if the network solution is included in the iterations as well. This could be a worthwhile option, not only for machines, but for other nonlinear or time-varying elements as well.

8.6 Saturation

Saturation effects in synchronous machines can have an influence on load flow, on steady-state and transient stability, and on electromagnetic transients. While transformer saturation usually causes more problems than machine saturation (e.g., in the creation of so-called "temporary overvoltages"), there are situations where saturation in machines must be taken into account, too.

To model machine saturation rigorously is very difficult. It would require magnetic field calculations, e.g.

by finite element methods [181], which is already time-consuming for one particular operating condition, and practically impossible for conditions which change from step to step. Also, the detailed data for field calculations would not be available to most EMTP users. An approximate treatment of saturation effects is, therefore, commonly accepted. The modelling of saturation effects is discussed in four parts,

(a) basic assumptions,

(b) saturation effects in steady-state operation, and

(c) saturation effects under transient conditions, and

(d) implementation in the EMTP

8.6.1 Basic Assumptions

The data which is normally available is the "open-circuit saturation curve" (Fig. 8.17), which shows the terminal voltage as a function of the field current for open-circuited armature windings (no-load condition). In the transient simulation, a flux-current relationship is required, rather than $V = f(i_f)$. This is easily obtained from Eq. (8.9), which becomes

$$v_q = \omega \lambda_d \tag{8.111a}$$

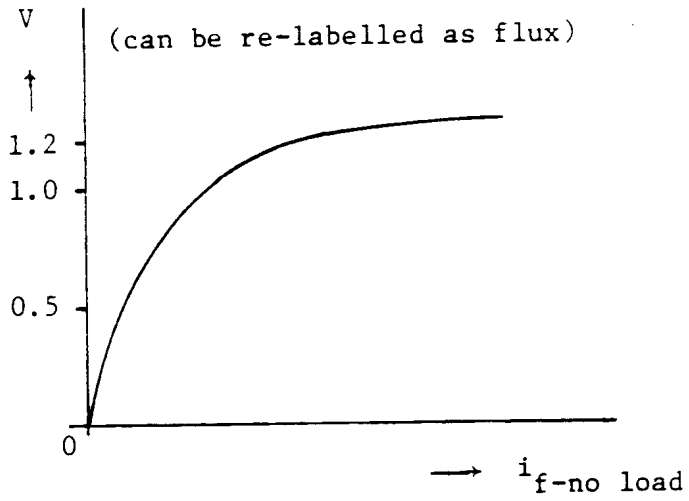

Fig. 8.17 - Open-circuit saturation curve

for balanced, open-circuit steady-state conditions, where both λ_q and the transformer voltages $d\lambda_d/dt$, $d\lambda_q/dt$ are zero. Since v_q is equal to $\sqrt{3}V_{1\text{-RMS}}$, this equation can be rewritten as

$$\sqrt{3}\, V_{1\text{-}RMS} = \omega \lambda_d \tag{8.111b}$$

where $V_{1\text{-RMS}}$ is the RMS terminal voltage of armature winding 1 (line-to-ground RMS voltage for wye-connected machines). It is therefore very simple to re-label the vertical axis in Fig. 8.17 from voltage to flux values with Eq. (8.111).

The saturation effects in synchronous machines do not produce harmonics during balanced steady-state

operation, because the open-circuit saturation curve describes a dc relationship between the dc flux of the rotating magnets (poles) and the dc field current required to produce it. The magnitude of the dc flux determines the magnitude of the induced voltages in the armature, while the shape of the flux distribution across the pole face determines the waveshape of the voltage. If the distribution is sinusoidal, as assumed in the ideal machine implemented in the EMTP, then the voltage will be sinusoidal as well. In reality, the distribution is distorted with "space harmonics," and it is this effect which produces the harmonics in synchronous machines.

There are many different ways of representing saturation effects [182], and it is not completely clear at this time which one comes closest to field test results. More research on this topic is needed. At this time, the representation of saturation effects in the EMTP is based upon the following simplifying assumptions:

1. The flux linkage of each winding in the d- or q-axis can be represented as the sum of a leakage flux (which passes only through that winding) and of a mutual flux (which passes through all other windings on that axis as well), as illustrated in Fig. 8.18,

$$\lambda = \lambda_{\sigma} + \lambda_m \tag{8.112}$$

where

λ_{σ} = leakage flux unaffected by saturation,

λ_m = mutual flux subjected to saturation effects.

In reality, the leakage fluxes are subjected to saturation effects as well because they pass partly through iron [180], but to a much lesser degree than the mutual flux. Saturation effects are therefore ignored in the leakage fluxes. The data is not available anyhow if only one saturation curve (open-circuit saturation curve) is given. In terms of equivalent circuits, this assumption means that only some of the inductances are nonlinear (shunt branch in star point in Fig. 8.2), while the others remain constant.

2. The degree of saturation is a function of the total air-gap flux linkage $\lambda_{m\text{-}u}$,

$$\lambda_m = f(\lambda_{m-u}) \tag{8.113a}$$

with

$$\lambda_{m-u} = \sqrt{\lambda_{md-u}^2 + \lambda_{mq-u}^2} \tag{8.113b}$$

and

$$\lambda_{md-u} = M_{du}(i_d + i_f + i_D)\,; \qquad \lambda_{mq-u} = M_{qu}(i_q + i_g + i_Q) \tag{8.113c}$$

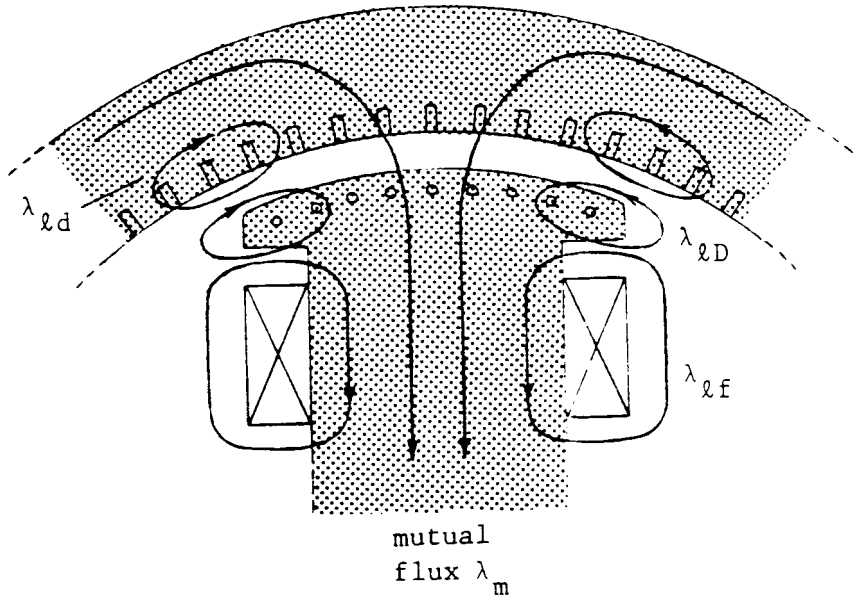

Fig. 8.18 - Leakage fluxes and mutual flux

where subscript "m" indicates mutual, and "u" indicates unsaturated values. In Eq. (8.113c) it is important to use the proper mutual inductances for the representation of the mutual flux. This leads back to the data conversion problem discussed in Section 8.2. If Canay's characteristic reactance X_c is not known, then assume k = 1 in Eq. (8.14b), and use

$$M_{du} = L_d - L_\sigma ; \qquad M_{qu} = L_q - L_\sigma$$

from Eq. (8.20a) and (8.20c). In this case, the equivalent star circuit of Fig. 8.2 shows the correct separation into the mutual inductance $M_m = M_{du}$ or M_{qu} for the mutual flux (subject to saturation) and into the leakage inductances for the leakage fluxes (linear d-, f-, and D-branches). If Canay's characteristic reactance is used, then Fig. 8.2 can no longer be used, as explained in Section 8.6.5.

3. Only one flux, namely the total air-gap flux, is subjected to saturation. The saturated mutual fluxes λ_{md}, λ_{mq} on both axes are found from their unsaturated values by reducing them with the same ratio (similar triangles in Fig. 8.19),

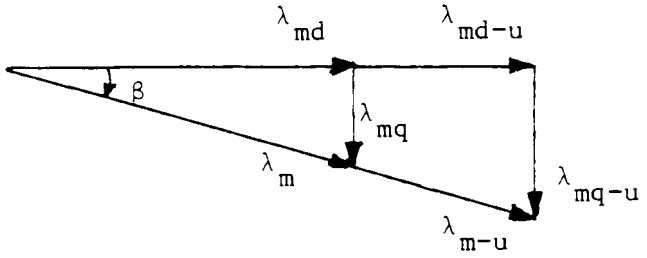

Fig. 8.19 - Unsaturated and saturated mutual fluxes

$$\lambda_{md} = \lambda_{md-u} \cdot \frac{\lambda_m}{\lambda_{m-u}} ; \qquad \lambda_{mq} = \lambda_{mq-u} \cdot \frac{\lambda_m}{\lambda_{m-u}} \tag{8.114}$$

This assumption is based on the observation that there is only one mutual flux, which lines up with the pole axis if λ_{mq} is very small, and which will shift to one side of the pole as λ_{mq} increases (Fig. 8.20).

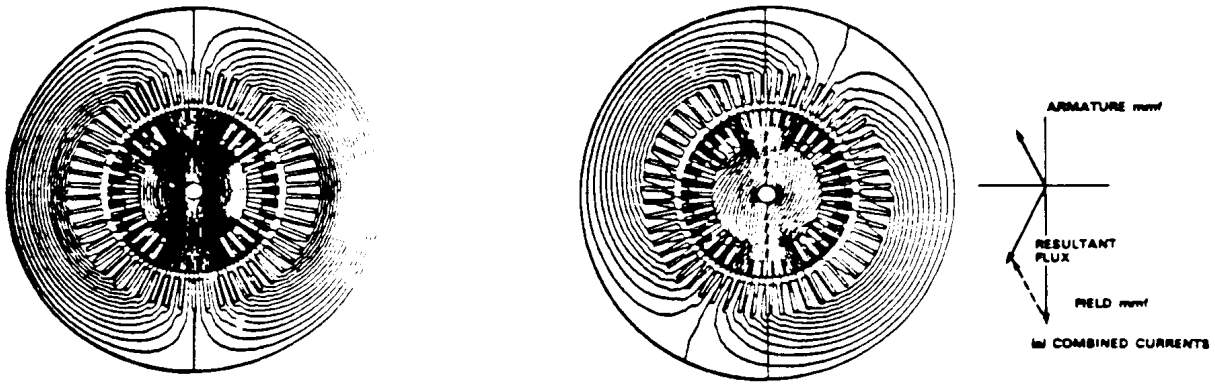

(a) flux from i_f alone ($\lambda_{mq} = 0$) (b) flux from i_f and stator currents $\lambda_{mq} \neq 0$

Fig. 8.20 - Flux in turbogenerator [181]. © 1981 IEEE

4. Saturation does not destroy the sinusoidal distribution of the magnetic field over the face of the pole, and all inductances therefore maintain their sinusoidal dependence on rotor position according to Eq. (8.5).
5. Hysteresis is ignored, while eddy currents are approximately modelled by the g-winding, and maybe to some extent with the D- and Q-windings. More windings could be added, in principal, to represent eddy currents more accurately.

8.6.2 Saturation in Steady-State Operation

At this time, the saturation effects are only modelled correctly in the ac steady-state initialization if the terminal voltages and currents are balanced. More research is needed before saturation can be represented properly in unbalanced cases.

As explained in Section 8.4, the initialization of the machine variables follows after the phasor steady-state solution of the complete network. The initialization for balanced (positive sequence) conditions is described in detail in Section 8.4.1, and only the modifications required to include saturation effects will be discussed here.

The nonlinear characteristic of Fig. 8.17 makes it impossible to use the initialization procedure of Section 8.4.1 in a straightforward way. To get around this problem, it is customary to use an "equivalent linear machine" in steady-state analysis which gives correct answers at the particular operating point and approximate answers in the neighborhood. This equivalent linear machine is represented by a straight line through the operating point and the origin (dotted line in Fig. 8.21). Whenever the operating point moves, a new straight line through the new operating point must be used.

The concept of the equivalent linear machine is used in the EMTP as follows.

1. Obtain the ac steady-state solution of the complete network. From the terminal voltages and currents of the

machine (positive sequence values), find the internal machine variables with the method of Section 8.4.1. Assume that the machine operates in the unsaturated region at this time.

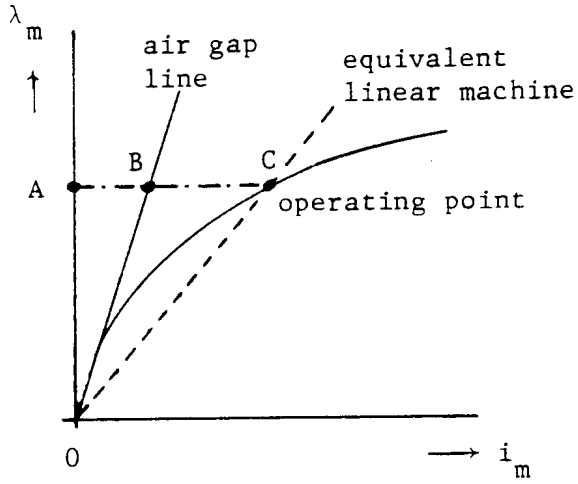

Fig. 8.21 - Linearization for steady-state analysis

2. Determine the total magnetizing current

$$i_m = \sqrt{(i_d + i_f + i_D)^2 + \left(\frac{M_{qu}}{M_{du}}\right)^2 (i_q + i_g + i_Q)^2} \tag{8.115a}$$

with i_D, i_g i_Q being zero for balanced conditions. Eq. (8.115) assumes turns ratios of $N_d:N_f:N_D = 1:1:1$ (same for quadrature axis). If any other turns ratios are used, the first term would be

$$M_{du} i_{md} = M_{du} i_d + M_{df-u} i_f + M_{dD-u} i_D \tag{8.115b}$$

and the second term

$$M_{qu} i_{mq} = M_{qu} i_q + M_{qg-u} i_g + M_{qQ-u} i_Q \tag{8.115c}$$

with

$$M_{du} i_m = \sqrt{(M_{du} i_{md})^2 + (M_{qu} i_{mq})^2} \tag{8.115d}$$

Find the operating point on the nonlinear characteristic of Fig. 8.21. If this point lies in the linear region, then the initialization is complete. Otherwise:

3. Calculate the ratio K from Fig. 8.21,

$$K = \frac{AB}{AC} \tag{8.116a}$$

and multiply the unsaturated mutual inductances with that ratio to obtained the saturated values of the equivalent linear machine,

$$M_d = K \cdot M_{du} \; ; \qquad M_q = K \cdot M_{qu} \tag{8.116b}$$

Use these values to repeat the initialization procedure of Section 8.4.1. Then re-calculate the magnetizing current from Eq. (8.115). If it agrees with the previously calculated value within a prescribed tolerance, then the initialization is finished. If not, repeat step 3. Convergence is usually achieved with 1 to 2 iterations of step 3.

In the BPA EMTP steady-state solution, machines are now represented as voltage sources at the terminals, and the terminal currents are obtained from that solution. With terminal voltages and currents thus known, their positive sequence components can be calculated and then used to correct the internal variables for saturation effects. Since this correction does not change the terminal voltages and currents, the complete network solution does not have to be repeated in step 3.

This will also be true in future versions of the EMTP, where the machine will be represented as symmetrical voltage sources behind an impedance matrix. Again, the terminal voltages and currents and their positive sequence components will be known from the steady-state solution.

In unbalanced cases, the present representation will produce negative sequence values, while the future representation will produce correct values. How to use these negative sequence values in the saturation corrections has not yet been worked out. Since they produce second harmonics in the direct and quadrature axes fluxes, it may well be best to ignore saturation effects in the negative sequence initialization procedure of Section 8.4.2 altogether.

The equivalent linear machine produces correct initial conditions for the different model used in the transient simulation, as can easily be verified if a steady-state solution is followed by a transient simulation without any disturbance.

8.6.3 Saturation under Transient Conditions

The equivalent linear machine described in Section 8.6.2 cannot be used in the transient solution, because the proper linearization for small disturbances (as they occur from step to step) is not the straight line 0-C in Fig. 8.21 ("linear inductance"), but the tangent to the nonlinear curve in point C ("incremental inductance").

The saturation effect enters the transient solution discussed in Section 8.5 in two places, namely through the speed voltages and through the transformer voltages. Consider the direct axis equations (8.76) first, which can be rewritten as

$$[v] = -[R][i] - \frac{d}{dt}\begin{bmatrix}\lambda_{\sigma d}\\ \lambda_{\sigma f}\\ \lambda_{\sigma D}\end{bmatrix} - \frac{d}{dt}\begin{bmatrix}\lambda_{md}\\ \lambda_{md}\\ \lambda_{md}\end{bmatrix} + \begin{bmatrix}-\omega\lambda_{\sigma q}\\ 0\\ 0\end{bmatrix} + \begin{bmatrix}-\omega\lambda_{mq}\\ 0\\ 0\end{bmatrix} \tag{8.117}$$

for the d, f, D-quantities if each flux linkage is separated into its leakage flux and the common mutual flux,

$$\begin{aligned}\lambda_d &= \lambda_{\sigma d} + \lambda_{md}\\ \lambda_f &= \lambda_{\sigma f} + \lambda_{md}\\ \lambda_D &= \lambda_{\sigma D} + \lambda_{md}\end{aligned} \tag{8.118}$$

assuming turns ratios of N_d:N_f:N_D = 1:1:1 (analogous for quadrature axis). Only the terms with λ_{md} and λ_{mq} in Eq. (8.117) are influenced by saturation, and only those terms are therefore discussed.

Consider first the speed voltage term $-\omega\lambda_{mq}$ in Eq. (8.117), which is properly corrected for saturation by simply using the correct saturated value λ_{mq}. The saturation correction has already been described in Eq. (8.114), and is conceptually the same as the one used in Eq. (8.116) for the steady-state solution. Since the transient solution works with predicted values of speed voltages $\omega\lambda_d$ and $\omega\lambda_q$, as explained in Section 8.5.4.4, they are used directly in Eq. (8.117) (not split up into two terms).

Next consider the transformer voltages $-[d\lambda_{md}/dt]$ in Eq. (8.117), where incremental changes ("incremental inductances") are important. By using the tangent of the nonlinear characteristic in the last solution point, one can linearize the flux-current relationship to

$$\lambda_m = \lambda_{knee} + M_{slope}\, i_m \tag{8.119}$$

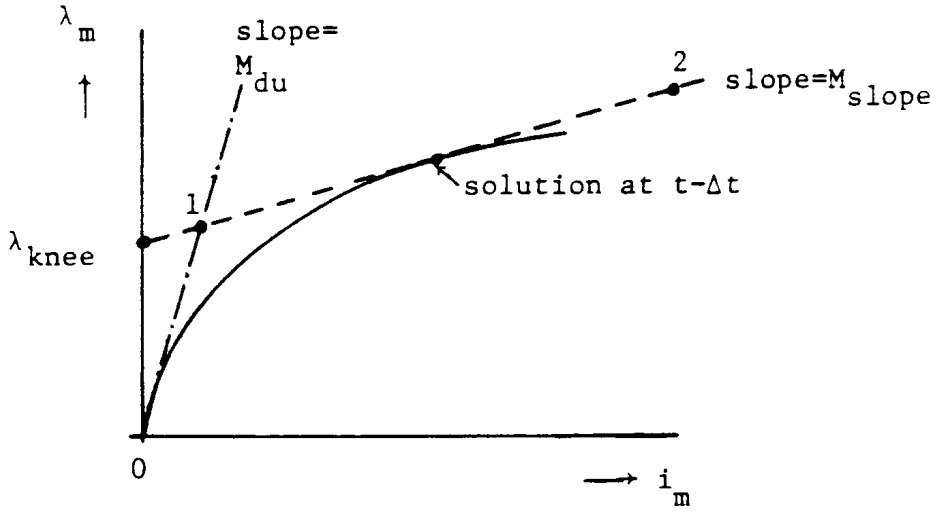

Fig. 8.22 - Linearization around last solution point

with M_{slope} being an incremental inductance (Fig. 8.22). This equation can be used over the next time step, because

the fluxes change only very slowly with typical step sizes of 50 to 500 μs. In the EMTP implementation, the problem is even simpler because the saturation curve is represented as a two-slope piecewise linear curve. In that case, the linearization of Eq. (8.119) changes only at the instant where the machine goes into saturation, and at the instant when it comes out again. With Eq. (8.113) and (8.115), the unsaturated total flux is

$$\lambda_{m-u} = M_{du}\, i_m \tag{8.120}$$

which, inserted into Eq. (8.119), produces

$$\lambda_m = \lambda_{knee} + b\,\lambda_{m-u} \tag{8.121a}$$

with the ratio between incremental inductance M_{slope} and linear (unsaturated) inductance M_{du},

$$b = \frac{M_{slope}}{M_{du}} \tag{8.121b}$$

After saturation has been defined for the total flux, it must be separated into d- and q-components again. With assumption (3) from Section 8.6.1, and with Fig. 8.19,

$$\begin{aligned} \lambda_{md} &= \lambda_{knee-d} + b\,\lambda_{md-u} \\ \lambda_{mq} &= \lambda_{knee-q} + b\,\lambda_{mq-u} \end{aligned} \tag{8.122a}$$

where

$$\lambda_{knee-d} = \lambda_{knee}\cos\beta\,; \quad \lambda_{knee-q} = \lambda_{knee}\sin\beta\,; \quad \beta = \tan^{-1}(\lambda_{mq-u}/\lambda_{md-u}) \tag{8.122b}$$

If Eq. (8.117), and the analogous equation for the quadrature axis, are solved with the trapezoidal rule of integration, then the transformer voltage term affected by saturation,

$$[v_{md}] = -\,d[\lambda_{md}]/dt$$

is transformed with Eq. (8.122) into

$$[v_{md}(t)] = -\frac{2b}{\Delta t}\{[\lambda_{md-u}(t)] - [\lambda_{md-u}(t-\Delta t)\} - \frac{2}{\Delta t}\{[\lambda_{knee-d}(t)] - [\lambda_{knee-d}(t-\Delta t)\} - [v_{md}(t-\Delta t)] \tag{8.123}$$

This equation shows how the transformer voltages must be corrected for saturation effects:

(a) multiply all mutual inductances by the factor b, and

(b) add correction terms to account for the variation of the knee fluxes [$\lambda_{knee\text{-}d}$], and [$\lambda_{knee\text{-}q}$]

8.6.4 Implementation in the EMTP

Saturation effects were modelled for the first time in the M27 version of the BPA EMTP, based on the concept of two independent saturation effects, one in the direct axis and the other in the quadrature axis. This was replaced with a newer model in the M32 version, which was essentially the model discussed here. It was not quite correct, however, because the correction terms in Eq. (8.123) related to the knee fluxes were not included. The model described here was implemented for the first time in the DCG/EPRI version to be released in 1986.

The open-circuit saturation curve is approximated as a two-slope piecewise linear characteristic (0-1 and 1-2 in Fig. 8.22). The number of linear segments could easily be increased, but a two-slope representation is usually adequate.

8.6.4.1 Steady-State Initialization

The initialization procedure is only correct for balanced networks at this time. The extension to unbalanced cases is planned for the future. Until this is done, some transients caused by incorrect initialization can be expected in unbalanced cases. Hopefully, they will settle down within the first few cycles.

The initialization follows the procedure of Section 8.6.2. For the reactances X_d, X_q, which consist of a constant leakage part and a saturable mutual part,

$$X_d = X_{\ell} + \omega M_d ; \qquad X_q = X_{\ell} + \omega M_q \tag{8.124}$$

unsaturated values M_{du}, M_{qu} are first used to obtain the internal machine variables with the method of Section 8.4.1. If the resulting magnetizing current lies in the saturated region, then the mutual reactances M_d, M_q in Eq. (8.124) must be corrected with Eq. (8.116). The calculation of the internal machine variables is then repeated with saturated reactances one or more times, until the changes in the magnetizing current become negligibly small.

With the two-slope piecewise linear representation implemented in the EMTP, the ratio K needed in Eq. (8.116) is

$$K = \frac{M_{slope}\, i_m + \lambda_{knee}}{M_{du}\, i_m} \tag{8.125}$$

with the meaning of the parameters shown in Fig. 8.22, and with i_m calculated from Eq. (8.115).

8.6.4.2 Transient Solution

Saturation effects in the time step loop are modelled according to Section 8.6.3. The coefficient b of Eq. (8.121b) is set to 1.0 in the unsaturated region, and to M_{slope}/M_{du} in the saturated region. Whenever the solution moves from one region into the other, it is reset accordingly.

This coefficient b affects the values in the equivalent resistance matrix [R_{equiv}] of Eq. (8.91a) and in the history term matrix of Eq. (8.82c). To include this coefficient, the inductance matrix of Eq. (8.76) is split up into

$$[L] = b\begin{bmatrix} L_{md-u} & L_{md-u} & L_{md-u} \\ L_{md-u} & L_{md-u} & L_{md-u} \\ L_{md-u} & L_{md-u} & L_{md-u} \end{bmatrix} + \begin{bmatrix} L_{\ell d} & & \\ & L_{\ell f} & \\ & & L_{\ell D} \end{bmatrix} \tag{8.126}$$

(analogous for quadrature axis). Whenever b changes, [L] is recalculated and then used to recalculate $[R_{equiv}]$ and the history term matrix of Eq. (8.82c). With the two-slope representation implemented in the EMTP, there are only two values of b, and the matrices could therefore be precalculated outside the time step loop for the two values of $b = 1$ and $b = M_{slope}/M_{du}$. The major effort lies in the re-triangularization of the network conductance matrix [G] of Eq. (8.18), however, which contains $[R_{equiv}]^{-1}$ and therefore changes whenever the machine moves into the saturated region, or out of it.

An additional modification is required in the calculation of the history terms with Eq. (8.78b). As shown in Eq. (8.123), the knee fluxes $\lambda_{knee}(t)$ and $\lambda_{knee}(t - \Delta t)$ must now be included. Since the trapezoidal rule of integration is not very good for the calculation of derivatives, the knee fluxes are included with the backward Euler method. First, the knee fluxes $\lambda_{knee\text{-}d}(t)$ and $\lambda_{knee\text{-}q}(t)$ are predicted, using the three-point predictor of Eq. (8.106). Then the trapezoidal rule expression

$$\frac{2}{\Delta t}\{[\lambda_{knee-d}(t)] - [\lambda_{knee-d}(t - \Delta t)]\}$$

is replaced with the backward Euler expression

$$\frac{1}{\Delta t}\{[\lambda^{predicted}_{knee-d}(t)] - [\lambda_{knee-d}(t - \Delta t)]\} \tag{8.127}$$

and the voltage term $[v_{md}(t - \Delta t)]$ is replaced by a voltage term which excludes the knee flux.

8.6.5 Saturation Effects with Canay's Characteristic Reactance

If saturation is ignored, then it does not matter whether Canay's characteristic reactance is used or not, because it only affects the data conversion part. With saturation included, however, the nonlinear inductance can only be identified as the shunt branch M_m in Fig. 8.2 if $k = 1$ in Eq. (8.14b). If Canay's characteristic reactance is known, then $k \neq 1$. This factor k must then be removed again from the rotor quantities in Eq. (8.15a), by multiplying the second and third row and column with its reciprocal value,

$$\begin{bmatrix} \lambda_d \\ \frac{\sqrt{3}}{\sqrt{2}}\lambda_f \\ \frac{\sqrt{3}}{\sqrt{2}}\lambda_D \end{bmatrix} = \begin{bmatrix} L_d & cM_m & cM_m \\ cM_m & c^2L_{ffm} & c^2M_m \\ cM_m & c^2M_m & c^2L_{DDm} \end{bmatrix} \begin{bmatrix} i_d \\ \frac{\sqrt{2}}{\sqrt{3}}i_f \\ \frac{\sqrt{2}}{\sqrt{3}}i_D \end{bmatrix} \tag{8.128}$$

where

$$c = \frac{1}{k} \tag{8.129}$$

and where M_m, L_{ffm} and L_{DDm} are the modified parameters straight out of the data conversion routine of Appendix VI.4. As explained in the text between Eq. (8.17) and (8.18), the factor $\sqrt{3}/\sqrt{2}$ in Eq. (8.128) is needed to produce turns ratios of $N_d:N_f:N_D = 1:1:1$. Only with turns ratios of 1:1 can the fluxes be separated into their main and leakage parts. The circuit of Fig. 8.23, which is equivalent to Eq. (8.128), has the correct separation into the mutual inductance $cM_m = 3/2\ M_{af}$ subjected to saturation (for the mutual flux), and into the linear leakage

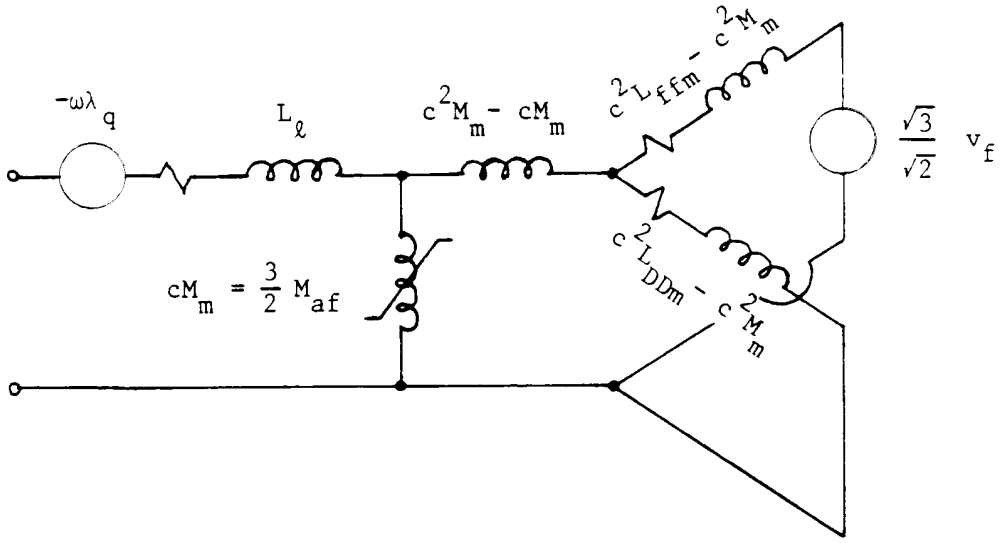

Fig. 8.23 - Equivalent circuit for direct axis with identity of leakage and main fluxes restored from Fig. 8.2

inductances in the three branches d, f, D. For the quadrature axis, Fig. 8.2 can still be used, with M_m being the nonlinear inductance, because Canay's characteristic reactance cannot be measured on that axis (current split between g- and Q-windings unmeasurable because both windings are hypothetical windings).

Most EMTP users will not know Canay's characteristic reactance because it is not supplied with the standard test data. Therefore, it has not yet been included in the saturation model in the EMTP, e.g. in the form of Fig. 8.23, because of lower priority compared to other issues. When it is implemented, one would have to decide whether the inductance $c^2M_m - cM_m$, which is mutual to both f- and D- windings, should be constant or saturable as well.